

NASA/CR—2004-213068



Planetary Transmission Diagnostics

Paul D. Samuel, Joseph K. Conroy, and Darryll J. Pines
University of Maryland, College Park, Maryland

May 2004

The NASA STI Program Office . . . in Profile

Since its founding, NASA has been dedicated to the advancement of aeronautics and space science. The NASA Scientific and Technical Information (STI) Program Office plays a key part in helping NASA maintain this important role.

The NASA STI Program Office is operated by Langley Research Center, the Lead Center for NASA's scientific and technical information. The NASA STI Program Office provides access to the NASA STI Database, the largest collection of aeronautical and space science STI in the world. The Program Office is also NASA's institutional mechanism for disseminating the results of its research and development activities. These results are published by NASA in the NASA STI Report Series, which includes the following report types:

- **TECHNICAL PUBLICATION.** Reports of completed research or a major significant phase of research that present the results of NASA programs and include extensive data or theoretical analysis. Includes compilations of significant scientific and technical data and information deemed to be of continuing reference value. NASA's counterpart of peer-reviewed formal professional papers but has less stringent limitations on manuscript length and extent of graphic presentations.
- **TECHNICAL MEMORANDUM.** Scientific and technical findings that are preliminary or of specialized interest, e.g., quick release reports, working papers, and bibliographies that contain minimal annotation. Does not contain extensive analysis.
- **CONTRACTOR REPORT.** Scientific and technical findings by NASA-sponsored contractors and grantees.

- **CONFERENCE PUBLICATION.** Collected papers from scientific and technical conferences, symposia, seminars, or other meetings sponsored or cosponsored by NASA.
- **SPECIAL PUBLICATION.** Scientific, technical, or historical information from NASA programs, projects, and missions, often concerned with subjects having substantial public interest.
- **TECHNICAL TRANSLATION.** English-language translations of foreign scientific and technical material pertinent to NASA's mission.

Specialized services that complement the STI Program Office's diverse offerings include creating custom thesauri, building customized databases, organizing and publishing research results . . . even providing videos.

For more information about the NASA STI Program Office, see the following:

- Access the NASA STI Program Home Page at <http://www.sti.nasa.gov>
- E-mail your question via the Internet to help@sti.nasa.gov
- Fax your question to the NASA Access Help Desk at 301-621-0134
- Telephone the NASA Access Help Desk at 301-621-0390
- Write to:
NASA Access Help Desk
NASA Center for Aerospace Information
7121 Standard Drive
Hanover, MD 21076

NASA/CR—2004-213068



Planetary Transmission Diagnostics

Paul D. Samuel, Joseph K. Conroy, and Darryll J. Pines
University of Maryland, College Park, Maryland

Prepared under Contract NAS3-2223

National Aeronautics and
Space Administration

Glenn Research Center

May 2004

Acknowledgments

This work is supported by the NASA Glenn Research Center, contract number NAS3-2223, with Dr. David G. Lewicki serving as the contract monitor.

Available from

NASA Center for Aerospace Information
7121 Standard Drive
Hanover, MD 21076

National Technical Information Service
5285 Port Royal Road
Springfield, VA 22100

Available electronically at <http://gltrs.grc.nasa.gov>

Planetary Transmission Diagnostics

Paul D. Samuel,* Joseph K. Conroy,† and Darryll J. Pines‡

University of Maryland

College Park, Maryland 20742

ABSTRACT

This report presents a methodology for detecting and diagnosing gear faults in the planetary stage of a helicopter transmission. This diagnostic technique is based on the constrained adaptive lifting algorithm. The lifting scheme, developed by Wim Sweldens of Bell Labs, is a time domain, prediction-error realization of the wavelet transform that allows for greater flexibility in the construction of wavelet bases. Classic lifting analyzes a given signal using wavelets derived from a single fundamental basis function. A number of researchers have proposed techniques for adding adaptivity to the lifting scheme, allowing the transform to choose from a set of fundamental bases the basis that best fits the signal. This characteristic is desirable for gear diagnostics as it allows the technique to tailor itself to a specific transmission by selecting a set of wavelets that best represent vibration signals obtained while the gearbox is operating under healthy-state conditions. However, constraints on certain basis characteristics are necessary to enhance the detection of local wave-form changes caused by certain types of gear damage. The proposed methodology analyzes individual tooth-mesh waveforms from a healthy-state gearbox vibration signal that was generated using the vibration separation (synchronous signal-averaging) algorithm. Each waveform is separated into analysis domains using zeros of its slope and curvature. The bases selected in each analysis domain are chosen to minimize the prediction error, and constrained to have the same-sign local slope and curvature as the original signal. The resulting set of bases is used to analyze future-state vibration signals and the lifting prediction error is inspected. The constraints allow the transform to effectively adapt to global amplitude changes, yielding small prediction errors. However, local wave-form changes associated with certain types of gear damage are poorly adapted, causing a significant change in the prediction error. The constrained adaptive lifting diagnostic algorithm is validated using data collected from the University of Maryland Transmission Test Rig and the results are discussed.

* Graduate Research Assistant, E-mail: bytor@glue.umd.edu, Telephone: 301 405 1142

† Undergraduate Research Assistant, E-mail: conroyj@glue.umd.edu, Telephone 301 405 1142

‡ Associate Professor, E-mail: djpterp@glue.umd.edu, Telephone: 301 405 0263

1. INTRODUCTION

In recent years, much research has been devoted to the development of Health and Usage Monitoring (HUM) systems for rotorcraft. The promise of HUM systems is the ability to provide accurate information regarding the condition of various flight critical components. This information would allow scheduled maintenance intervals to be increased and minimize the number of parts decommissioned before the end of their useful life thus reducing operating costs associated with civilian and military helicopters. In addition, an increase in helicopter safety and reliability could be realized.

Typically, transmission diagnostic algorithms use vibration data collected from accelerometers located on the transmission housing. The vibration signals collected by these sensors tend to be composites of vibrations associated with all of the components within the transmission. To provide an accurate diagnosis of a fault in the transmission, it is necessary to understand which component within the transmission is causing a given vibration pattern.

Time domain averaging has been shown to be a useful tool for extracting gear mesh vibrations from composite vibration signals since it enables the extraction of periodic signals from noise-polluted signals. The implementation of this methodology is straight forward for fixed-axis gears. However, most helicopters have one or more planetary reduction stages incorporated in their transmissions. The complex motion of the planetary stage components, specifically the planet gears and sun gear, in conjunction with the requirement that all sensors remain external to the transmission, necessitates the incorporation of an additional processing step to isolate the vibrations associated with each individual component.

A technique for extracting the vibration signals associated with the sun and planet gears of a planetary gearbox was proposed by P.D. McFadden in the late 1980s (1; 2). This technique is referred to as vibration separation. His work demonstrates that, for planetary gearboxes with a hunting tooth ratio between the planet and ring gears and the sun and ring gears, these vibration signals can be extracted from a vibration signal captured by a single fixed-frame sensor. If multiple sensors can be placed on the gearbox housing such that the vibration signals obtained have a similar form, e.g. at different points about the ring gear, then an extension of McFadden's technique can be used to combine the signals(3). Combining vibrations signals from multiple sensors offers enhanced robustness to sensor failures, external disturbances and noise.

Once a useful signal has been obtained, analysis can be performed to determine whether evidence of gear damage is present in the signal. Many traditional rotating machinery diagnostic methodologies attempt to enhance changes in the statistical properties of the vibration data in order to detect damage(4; 5; 6; 7). However,

recent advancements in time-frequency analysis have resulted in more advanced diagnostic algorithms(8; 9; 10; 11) and fault classification algorithms(12; 13). These techniques are based primarily on wavelet analysis.

The advent of adaptive representations offers the potential to analyze a given vibration signal using a set of wavelet basis functions chosen from a set of fundamental wavelet bases that best represent the signal at each point. Hence, a change in perspective is suggested for diagnostic algorithms: instead of using the wavelet transform to exclusively investigate changes in the characteristics of a vibration signal, a set of wavelets can be chosen that best represent a signal obtained from a known operating condition, and this set of basis can then be compared to a signal obtained from the transmission during use(14). The set of basis can thus be considered to be a phenomenological model of the transmission vibration signal. In the ideal case, a physics-based model of the transmission would be used to generate expected vibration signals for various operating conditions. However, current physics-based models of planetary gear train dynamics (15) are still in the early stages of development and are insufficient for use in diagnostic algorithms.

In order to effectively generate a model of transmission vibration signals that exist in the time domain, a method to implement the wavelet transform in the time domain is desired. One such method is the lifting scheme (16), a time domain prediction-error realization of the wavelet transform. Methods for adding adaptivity to the lifting scheme have begun to be investigated(17; 18). The method used in this work is based on that developed by Claypoole, et al.(18). However, it has been found that, in general, adaptive lifting by itself is too flexible to allow the effective distinction of healthy-state and damaged-state vibration signals. Hence, it has been determined that constraints on certain basis characteristics are necessary to enhance the detection of local wave-form changes caused by certain types of gear damage. This processing technique is termed Constrained Adaptive Lifting (CAL).

This report describes the planetary transmission vibration separation algorithm and discusses the real-time implementation of the technique. A summary of the lifting scheme is presented and the incorporation of adaptivity and constraints to develop CAL is discussed. A diagnostic technique based on the CAL algorithm is developed. To validate the methodology, healthy-state and damaged-state data was collected from a planetary transmission test rig, the University of Maryland Transmission Test Rig (UMTTR), and preprocessed using the vibration separation algorithm. The results are then presented. A manual for the real time software is included in the appendix.

Helicopter Model	Transmission Configuration
Bell 206	2 Stage: Bevel and Planetary
Bell 206 Long Ranger	2 Stage: Bevel and Planetary
Bell 412 EP	3 Stage: 1 Spiral-Bevel and 2 Planetary
Bell 430	3 Stage: 2 Spiral-Bevel and 1 Planetary
Bell 407	2 Stage: Bevel and Planetary

Table 1. Transmission Configurations for Various Helicopters

2. PLANETARY TRANSMISSION VIBRATION SEPARATION

2.1. Introduction

Time synchronous averaging is a powerful signal processing technique for the extraction of a periodic waveform from data containing both noise and waveforms generated by other sources of excitation whose periods are not commensurate with the period of interest(19). This technique has been shown to be particularly useful for the analysis of the vibration of rotating machinery, and in particular, transmissions, since it enables the vibration of a single fixed-axis gear to be separated from the overall vibration of the transmission. The resulting vibration signal corresponds to one complete revolution of the gear under consideration, and thus changes in the vibration waveform due to damage on individual teeth can be identified. Often, changes due to extensive damage can be seen by direct inspection of the signal. However, for detection of incipient damage, additional signal processing techniques is necessary. Many of the current signal processing techniques used for transmission damage detection involve statistical averaging. It should be noted that the use of the time averaged vibration signal is implicit in the application of the majority of those diagnostic techniques. In addition, the techniques are typically validated exclusively on time averaged signals.

The implementation of a time synchronous averaging algorithm for fixed-axis gears is relatively straight forward. However, for helicopter transmission diagnostics, additional complexities are introduced. Most helicopters currently in operation have one or more planetary reduction stages included in their transmission. This is due to the load sharing properties of a planetary transmission configuration. Transmission configurations for various helicopters are given in Table 1.

The difficulty of extracting a time synchronous average from a planetary transmission stems from two factors. First, transducers may only be placed external to the transmission, typically on the transmission housing. Second, the rotational axes of the planet gears are not fixed, i.e. they move relative to the transmission housing and thus relative to the transducers. As a result, the vibration signal of the planet gear under consideration may be

distorted by the vibration signals from the other planet gears. This could cause a signal from a faulty planet gear to be masked by that of healthy planet gears. Thus, a separate technique for the extraction of the time averaged vibration signals associated with the individual planet gears and sun gear in a planetary transmission is required. This technique, herein referred to as *vibration separation*, was first reported by McFadden in the late 1980s(1; 2).

This section of the report will discuss issues involved in the application of time synchronous averaging to planetary transmissions. First, appropriate preparation of the vibration data will be considered. General synchronous averaging will then be presented. The additional complexities posed by the planetary transmission configuration will be discussed. The vibration separation technique used to obtain a synchronous average of the vibration signal generated by the individual planets gears and sun gear using a signal collected from a single transducer will be presented. An extension of the technique to include the use of multiple vibration transducers will be proposed and discussed. Finally, a comparison of various window functions is presented.

2.2. Data Conditioning for Synchronous Averaging

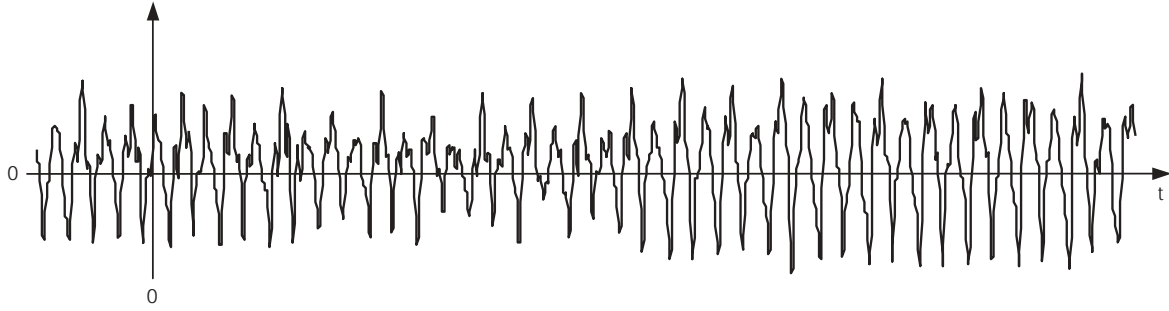
Prior to the application of synchronous averaging, the vibration signals collected from the transducer attached to the transmission housing must be conditioned, i.e. put into a form appropriate for digital signal processing. Conditioning involves two processes, digitization and interpolation.

2.2.1. Digitization

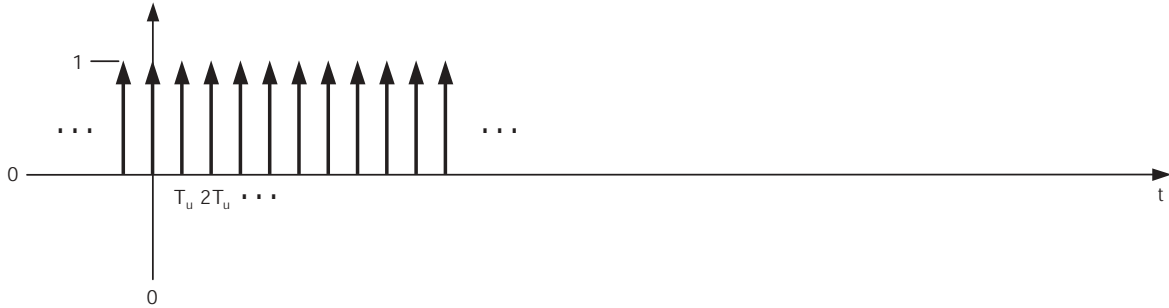
Transmission diagnostic techniques typically involve digital signal processing. Thus, vibration signals collected from the transducer must be converted to discrete-time digital signals prior to the application of the technique. This conversion, herein referred to as digitization, is performed using two processes, quantization and sampling. Quantization is generally handled by the data acquisition system. However, the analyst has more control over the choice of an appropriate sampling frequency, f_{sample} . Sampling can be represented as the multiplication of a continuous time signal $x(t)$ (see figure 1(a)) by an infinite series of impulses with a period $T_u = 1/f_{sample}$ (see figure 1(b)), referred to as the sampling function and given by

$$u(t) = \sum_{k=-\infty}^{\infty} \delta(t - kT_u) \quad (1)$$

The choice of sampling frequency is typically a tradeoff between the available processing power and memory of the digital signal processing system, and the requirement that the continuous-time analog vibration signal be accurately represented by its digital counterpart. A study of the effect of sampling rate on the performance



(a) Continuous-Time Signal $x(t)$



(b) Sampling Function $u(t)$

Figure 1. Sampling of a Continuous-Time Signal

of two damage detection metrics, FM4 and NA4, was performed by Decker and Zakrajsek in 1999(20). It was determined that for a set of spur gears, each with 28 teeth, operating at 10,000 revolutions per minute (rpm), a sampling rate of 125,000 samples per second (125 kHz) was desirable. More generally, this is equal to a sampling rate of approximately 26.8 samples for a single tooth mesh period, where the tooth mesh period is defined as seconds per tooth mesh, given by

$$\text{Tooth Mesh Period} = \frac{1}{\text{Number of Teeth} * \text{Rotational Frequency (Hz)}} \quad (2)$$

This result is considered to be a good rule of thumb for a minimum acceptable sampling rate. However, higher sampling rates, if available, may further improve performance.

2.2.2. Interpolation

Additional issues must be considered in the application of synchronous averaging to vibration signals sampled using a fixed sample rate. Synchronous averaging, discussed in in greater detail in Section 2.2.3, requires that the signal under consideration be divided into successive sections, where the duration of each section is equal to the period of interest. These sections can then be ensemble averaged. In the case of transmission vibration

signals, this period is one rotation of the gear being analyzed. Note that this period is not defined in terms of time, but in terms of rotational angle. One period is equal to 360 degrees of rotation of the gear, independent of time. However, the sampling frequency is fixed in time. Thus, for a given sampling frequency, the samples per rotation is a function of the rpm of the transmission.

To simply average two discrete time signals, the number of samples in each signal must be equal. However, synchronous averaging requires that the period of the signals be equal and that the signals be in phase. This implies that for transmission vibration signals, in order to extract the periodic waveform associated with a given gear, the angular position of the gear must be known, and the gear must remain at a constant rpm, since the number of samples per rotation is a function of rpm. In practice, it is possible to determine the angular position of the gear using a reference signal such as a one per revolution pulse generator attached to the gear shaft. However, it is not possible to hold the rpm of a transmission exactly constant. For instance, the rpm of a helicopter transmission will typically vary by one or two percent during normal operation(21).

The problem lies in the fact that the sampling frequency is defined in terms of time while the rotational period of the gear is defined in terms of angle. To overcome this problem some technique must be used to transform the vibration signal from the time domain to the angle domain, thus redefining the sampling frequency to be a function of angular position rather than time. This can most easily be accomplished through the use of interpolation. If the reference signal is sampled at the same rate as the vibration signal, then, for each sample of the vibration signal, the corresponding reference position is known. Interpolation can be used to bring the number of points sampled during one rotational period of the gear to a predetermined value, thus relating each point in the interpolated signal to some increment of the gears rotation, and enabling averaging.

For a helicopter transmission, a pulse generator providing one pulse per revolution of the output shaft is commonly available. This signal can be sampled and used as the reference signal. In this case, the position is known exactly only once per revolution. However, this is sufficient as it allows the vibration signal to be divided into sections corresponding to one output revolution of the transmission. These sections can then be interpolated to a predetermined value. This value is typically some power of two near the expected number of samples per revolution determined using the expected nominal operating rpm of the transmission. A power of two is chosen to simplify the application of subsequent signal processing techniques.

A number of interpolation techniques are available, so an understanding of the advantages and limitations of each technique is necessary in order to choose the most appropriate. In general, this choice is a tradeoff between accuracy and computational effort. In 1989, McFadden presented a comparison of sample-and-hold, linear and cubic interpolation(22). It was concluded that cubic interpolation was the most accurate, as its

frequency response had a flatter passband and smaller sidelobes in the stopband than the other two techniques. However, the accuracy advantage of cubic interpolation over linear interpolation was found to be slight, while the computational effort required was found to be significantly greater. Sample-and-hold interpolation was found to have insufficient accuracy. Thus, linear interpolation was determined to be the optimum choice. A second comparison was performed by Decker and Zakrajsek in 1999(20). For this study, linear, cubic and cubic spline interpolation were considered. Two diagnostic metrics, FM4 and NA4, were computed for vibration signals interpolated using the three techniques, and their performance was compared. In this case, only slight differences were reported in the output of the diagnostic metrics. However, the computational effort required by linear interpolation was shown to be significantly smaller than that required by the other two techniques. Thus, linear interpolation was again suggested.

It is important to note the fundamental assumption underlying this approach. *The application of interpolation to vibration signals obtained from a helicopter transmission assumes that variations in the rpm of the transmission are negligible during one rotation of the transmission.* This assumption has been accepted by the transmission diagnostics community.

2.2.3. Time Synchronous Averaging

Time synchronous averaging is a useful signal processing technique for the extraction of periodic waveforms from noisy data. Implementation requires that the signal under consideration be divided into successive sections, where the duration of each section is equal to the period of interest. Thus, either the period of the desired waveform must be known, or a reference signal synchronous with the desired waveform must be recorded. Once the signal has been successfully segmented, the sections can be ensemble averaged. Averaging tends to reduced the contributions of both noise and waveforms whose period is not commensurate with the period of interest.

In the case of transmission vibration signals, the period of interest is one rotation of the gear being analyzed. Sufficiently accurate knowledge of this period is generally not available given that small variations in operating rpm are common, while sampling generally occurs at a fixed clock frequency. Hence the use of a reference signal, typically a one per revolution pulse train, is necessary. To ensure that each data section consists of the same number of samples, interpolation must be used prior to averaging. Interpolation is discussed in Section 2.2.2. Once interpolation has been performed and an appropriate set of data sections has been obtained, averaging can commence.

Let the signal $y(t)$ be composed of the periodic waveform of interest $x(t)$ with a period T_g , and noise $e(t)$, given as

$$y(t) = x(t) + e(t) \tag{3}$$

By definition, the average, $a(t)$ is given as

$$a(t) = \frac{1}{N} \sum_{n=0}^{N-1} y(t + nT_g) \quad (4)$$

where N sections are ensemble averaged(23).

The application of this model of the averaging process to the extraction of periodic waveforms was proposed by Braun in the mid 1970's(19). The segmenting process can be represented by the convolution of the signal $y(t)$ with a sampling function $g(t)$, where $g(t)$ consists of a series of unit impulses $\delta(t + nT_g)$ with amplitude $1/N$ located at $t = -nT_g$ and given as

$$g(t) = \frac{1}{N} \sum_{n=0}^{N-1} \delta(t + nT_g) \quad (5)$$

The convolution of $y(t)$ with a single unit impulse $\delta(t + nT_g)$ causes $y(t)$ to be shifted in the direction of negative time by nT_g , yielding a shifted signal given by

$$y(t + nT_g) = y(t) * \delta(t + nT_g) \quad (6)$$

Thus, the convolution of $y(t)$ with the sampling function $g(t)$ is the sum of N shifted signals, each shifted by $nT_g, n = 0, 1, \dots, N - 1$, and given as

$$g(t) * y(t) = \frac{1}{N} \sum_{n=0}^{N-1} y(t + nT_g) \quad (7)$$

A comparison of equations 4 and 7 reveals that the time synchronous average is given by

$$a(t) = g(t) * y(t) \quad (8)$$

This model provides a sufficient description of the mechanics of time synchronous averaging. However, it is not directly applicable to vibration signals collected from a planetary transmission. In order to develop a technique for extracting averaged vibration signals associated with the individual planet and sun gears, the planetary transmission geometry must be considered.

2.2.4. Planetary Transmission Geometry

The implementation of a time synchronous averaging algorithm for fixed-axis gears is relatively straight forward. Averaging as presented in Section 2.2.3 can be directly applied. However, for a planetary transmission, additional complexities are introduced. The difficulty of extracting a time synchronous average from a planetary transmission stems from two factors. First, transducers may only be placed external to the transmission, typically on the transmission housing. Second, the rotational axes of the planet gears are not fixed, i.e. they move relative to the transmission housing and thus relative to the transducers. Before the technique for extracting the averaged

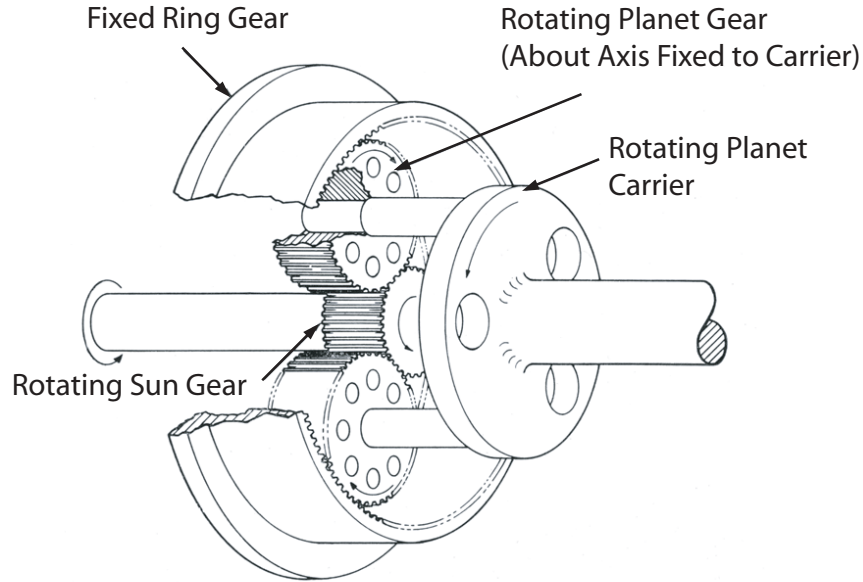


Figure 2. Planetary Transmission Schematic

vibration signatures of the individual components of a planetary transmission can be described, the geometry must be examined and important properties defined.

The planetary transmission configuration is a member of a larger class of transmission configurations known as epicyclic transmissions. An epicyclic transmission consists of a central sun gear, a ring gear with internal teeth, and a set of planet gears that mesh with both the sun gear and the ring gear, and whose rotational axes are fixed to relative to each other by the planet carrier. There are three configurations within the epicyclic class: the planetary, the star, and the solar configurations. Each is defined by which components are allowed to rotate and which are fixed relative to the transmission housing or fixed frame. In general, helicopter transmissions incorporate only the planetary transmission configuration. In a planetary transmission, the input shaft is attached to the sun gear, the output shaft is attached to the planet carrier, and the ring gear is fixed. A schematic of a typical planetary transmission is shown in figure 2.

The planetary configuration has two characteristics that make it particularly attractive for use in a helicopter transmission. First is load sharing. The input load is shared equally by each of the planets. Thus no one set of meshing teeth see the entire load being passed through the transmission. This enables relatively high reduction ratios to be attained at a relatively low rpm (high torque). Hence, the last stage of a helicopter transmission is typically a planetary stage. The second characteristic is the fixed ring gear. This is convenient as the ring gear

can be incorporated into the transmission housing.

From inspection of figure 2, it can now be seen that the planet gears move relative to any transducer placed on the transmission housing. In addition, sun gear vibrations can only be seen filtered through the planet gear. Given the geometry of the planetary transmission, specific properties of interest can now be defined.

The first property of interest in a planetary transmission is the tooth meshing frequency, f_m . Figure 3(a) shows a simple schematic of a planetary gearbox. The rotation frequency of the carrier is given as f_c and the rotation frequencies of the sun and planet relative to the carrier are given as f_s and f_p , respectively. To find the relationships between the rotation frequencies and the tooth mesh frequency, it is easiest to fix the planet carrier and let the ring gear rotate at a frequency equal to the carrier rotation frequency, as shown in figure 3(b). It is evident from inspection of this figure that the mesh frequency is given by

$$f_m = N_r f_c = N_p (f_p + f_c) = N_s (f_s - f_c). \quad (9)$$

where N_r , N_p and N_s are the number of teeth on the ring, planet and sun gears, respectively. From this equation, we can obtain the rotation frequency of the planet gear relative to the ring gear, $f_p + f_c$, and the sun gear relative to the ring gear, $f_s - f_c$, which are given by

$$f_p + f_c = f_c (N_r / N_p) \quad (10)$$

$$f_s - f_c = f_c (N_r / N_s) \quad (11)$$

respectively. From these equations, it can be seen that, more generally, the rotation frequency of the gear of interest is given by

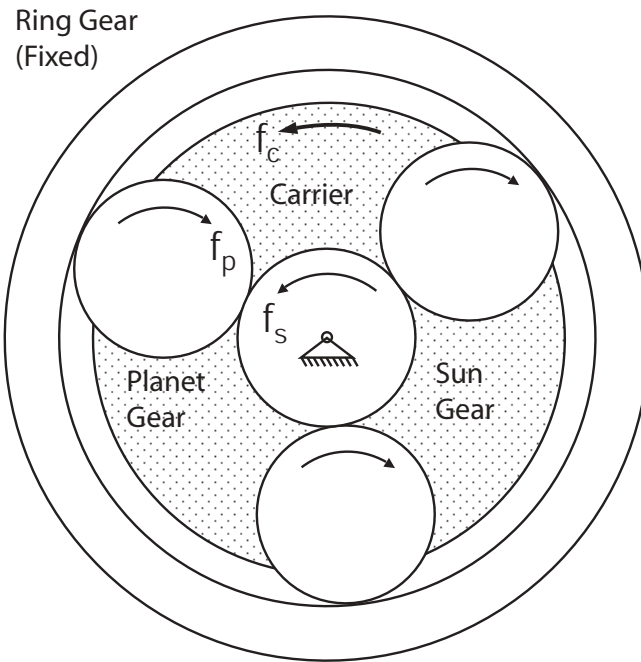
$$f_g = f_c (N_r / N_g) \quad (12)$$

where the subscript g refers to the gear under consideration, either the planet or the sun. Thus, the methodology presented is general to both the planet gears and sun gear and the subsequent development applies to a general gear.

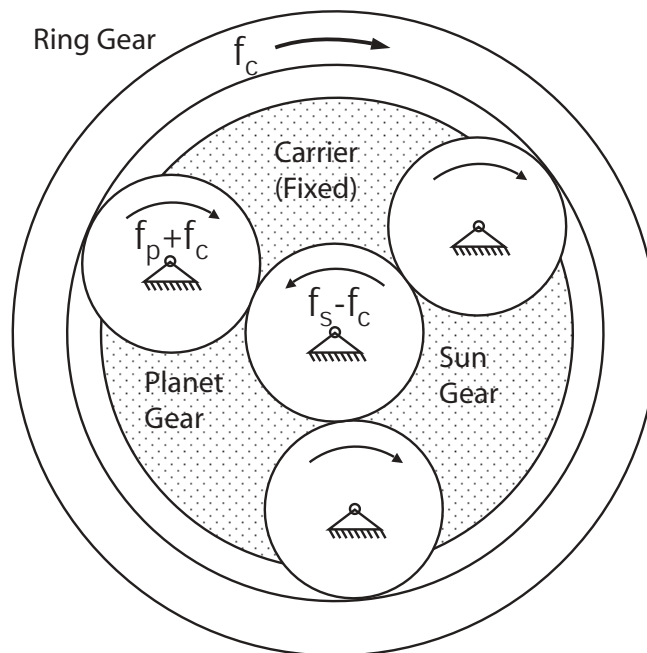
The next geometric property of interest is the number of rotations of the gear under consideration that occur before the gear returns to its initial state relative to the position of the carrier. This number of rotations, $n_{Reset,g}$, is given by

$$n_{Reset,g} = \frac{LCM(N_g, N_r)}{N_r} \quad (13)$$

where LCM refers to the least common multiple. In essence, a given tooth of a gear will be aligned (in the case of the planet gear, alignment implies meshing) with a given tooth of the ring gear for a given carrier orientation only once every $n_{Reset,g}$ rotations. If $n_{Reset,g} = 1$ then this gear state will occur once every carrier cycle at the



(a) Ring Gear Fixed.



(b) Carrier Fixed.

Figure 3. Planetary Transmission Rotational Frequencies.

given carrier orientation. However, if $n_{Reset,g} > 1$ then a sequence of gear states (one per carrier rotation) of length $n_{Reset,g}$ will occur at a given carrier orientation before the initial state is repeated. For each of these states, a different tooth of the gear will be aligned with a given ring tooth. Thus, the sequence of states has an associated sequence of aligned teeth. This sequence of teeth can be found using

$$P_{n,g} = \text{mod}(nN_r, N_g) + 1 \quad (14)$$

where the tooth aligned in the initial state, $P_{0,g}$, is defined as tooth 1. It can be seen that $P_{0,g} = P_{n_{Reset,g}}$.

It should be noted that for the planetary reduction stage of a typical helicopter transmission, $n_{Reset,p} = N_p$, i.e. each tooth of the planet gear will mesh with a given tooth of the ring gear before the initial planet tooth meshes with the ring tooth a second time. Under this condition, a hunting tooth ratio exists between the planets and ring teeth. This is done to ensure an even wear pattern during the life of the gearbox. However, it is not necessarily true that $n_{Reset,s} = N_s$.

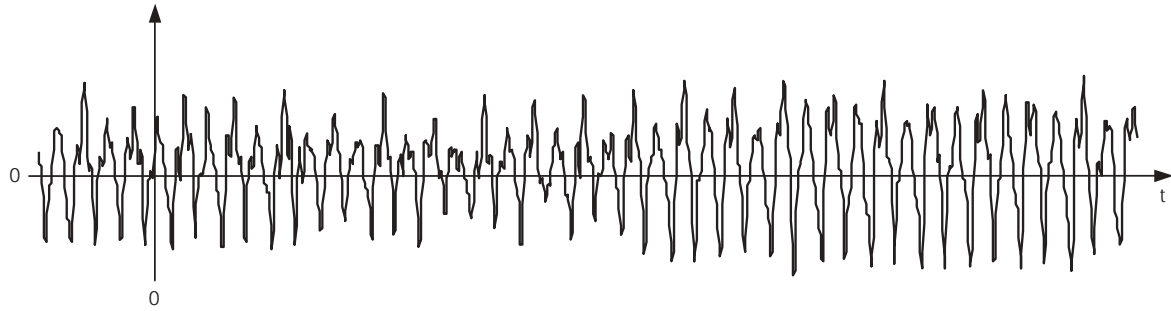
2.3. Vibration Separation for a Single Transducer

A technique for extracting the time averaged vibration signals associated with the sun and planet gears of a planetary gearbox was proposed by P.D. McFadden in the late 1980s (1; 2). This work demonstrates that, for planetary gearboxes with certain geometric properties, specifically $n_{Reset,p} = N_p$ and $n_{Reset,s} = N_s$, the averaged vibration signals can be extracted from a vibration signal captured by a single fixed-frame transducer. Subsequent studies validated this research and presented slight variations on the technique(24; 25; 3; 26). However, the fundamental methodology remains unchanged.

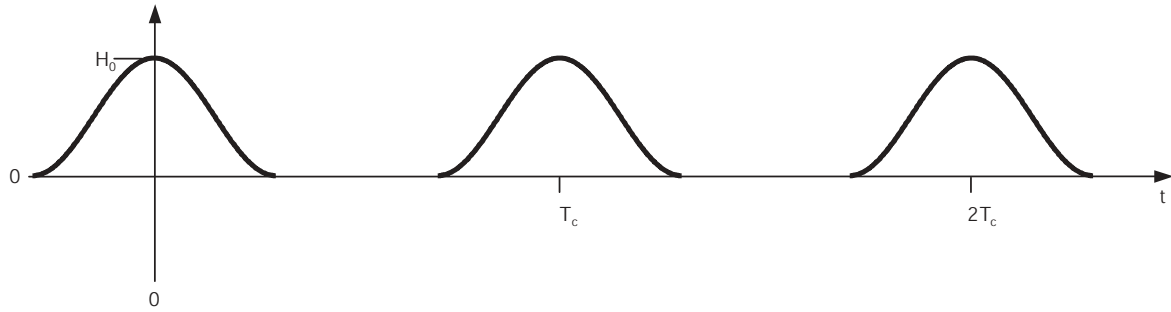
2.3.1. Theory

Let the continuous time vibration signal of a given planet gear associated with the meshing of the planet gear with the sun and ring gears be given by $x(t)$ as shown in figure 4(a). Typically, helicopter transmission vibration signals are measured using transducers, specifically accelerometers, mounted to the transmission housing. Consider an accelerometer, j , mounted on the circumference of the ring gear radially aligned with a given ring gear tooth, $P_{j,g}$ as shown in figure 5.

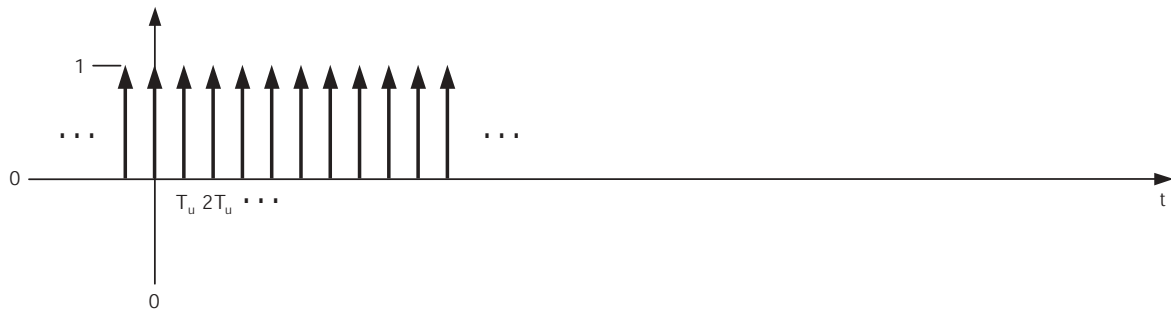
It has been shown that as a given planet gear approaches a transducer the level of vibration measured by the transducer increases, and then as the planet gear moves away from the transducer the level of vibration measured by the transducer decreases(27; 28). The transfer function between the transducer and the planet gear is given by $h(t)$ and has a period of one carrier rotation, T_c (see figure 4(b)). Hence, $x(t)$ as seen by accelerometer j is given by $h_j(t)x(t)$. The accelerometer signal is then sampled. Recall that sampling can be represented as



(a) Continuous Time Planet Vibration Signal $x(t)$



(b) Transfer Function Between Planet and Transducer $h(t)$



(c) Sampling Function $u(t)$

Figure 4. Elements of a Discrete-Time Planet Vibration Signal Measured by a Fixed Transducer

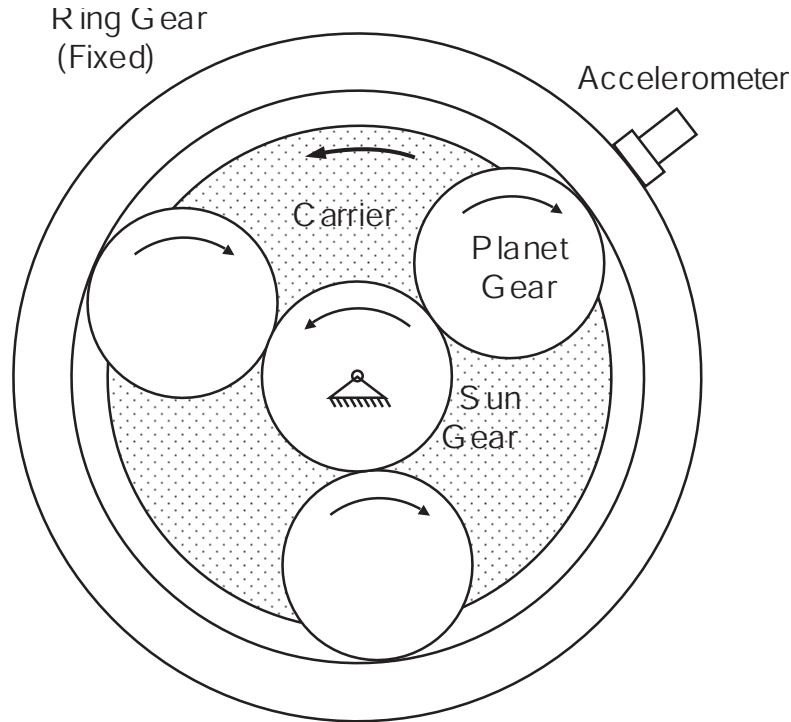


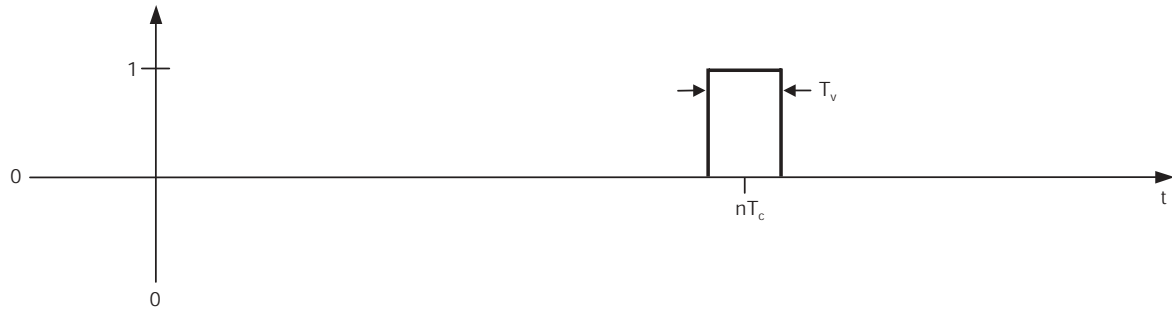
Figure 5. Transducer Position

multiplication by the sampling function $u(t)$ (see figure 4(c)). Thus, the final digitized vibration signal generated by the planet gear as seen by accelerometer j is given by $h_j(t)x(t)u(t)$.

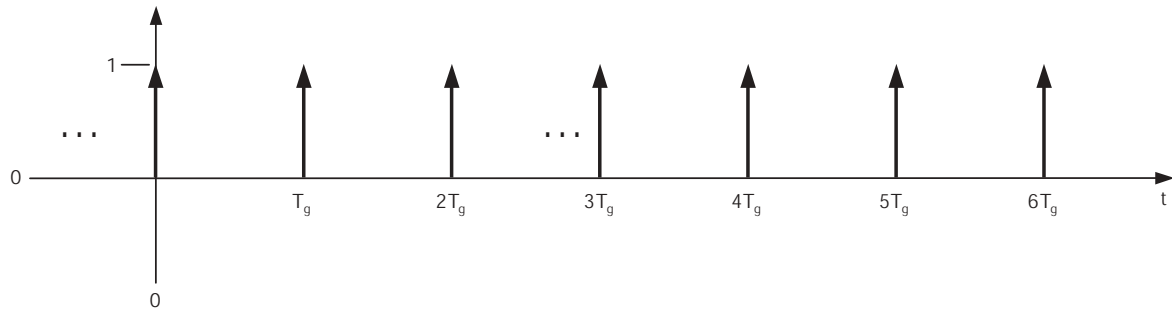
The underlying assumption behind the vibration separation technique can now be stated. *The fundamental assumption of the vibration separation algorithm is that when a given planet gear is near a transducer, the vibrations measured by the transducer are dominated by the meshing of that specific planet gear with the sun and ring gears.* It has been shown that by applying equation 14, the sequence of planet or sun gear teeth that pass a given fixed-frame accelerometer can be determined. Thus, if a small window of data is collected during each passing of a given planet, these windows can be mapped into their appropriate locations, based on the tooth pass sequence, to synthesize the vibration signal associated with a single rotation of the planet or sun gear. The window serves to attenuate vibrations not associated with the meshing of gear of interest. The mapping is performed by the application of basic synchronous averaging to the windowed vibration signal, using the period of rotation of the gear under consideration. This is the theory behind the vibration separation technique.

2.3.2. Methodology

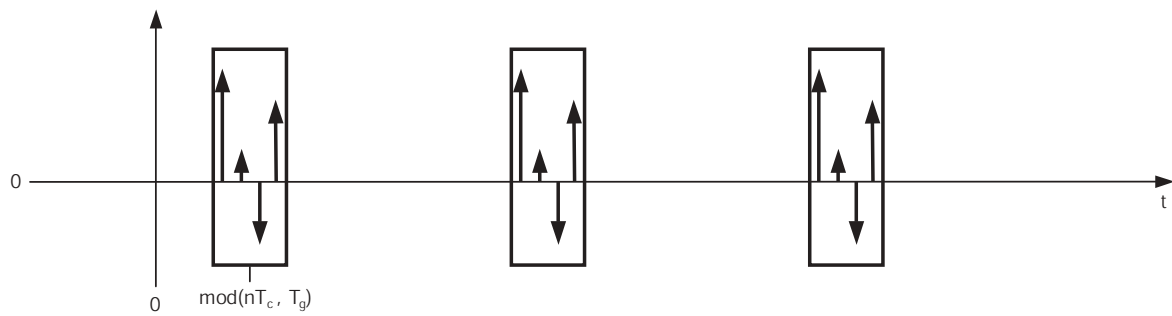
Formally, the vibration separation technique as applied to a discrete-time planet vibration signal collected from a single fixed-frame transducer is given as follows. Define the windowing function centered at time $t = nT_c$, the



(a) Windowing Function $v(t - nT_c)$



(b) Sampling Function $g(t)$ with Period T_g



(c) Windowed and Mapped Vibration Signal $[H_{j,0}x(t)u(t)v(t - nT_c)] * g(t)$

Figure 6. Planet Vibration Signal Windowing and Mapping

time at which $h_j(t)$ is a maximum, is defined as $v(t - nT_c)$ (see figure 6(a)). For simplicity, let the window be a rectangular function. The use of different window functions is discussed in detail in Section 2.5. Let the window width be chosen as an integer number of tooth mesh periods, given by

$$T_v = M_v T_m \quad (15)$$

The subsequent windowed vibration signal is given by the expression $h_j(t)x(t)u(t)v(t - nT_c)$. If M_v is chosen to be appropriately small, then the amplitude of $h(t)$ can be assumed to be a constant H_0 over the window, and thus

$$h_j(t)x(t)u(t)v(t - nT_c) = H_{j,0}x(t)u(t)v(t - nT_c). \quad (16)$$

Once a window of vibration data has been obtained, it must be mapped into the appropriate location in the synthesized gear vibration signal. To determine this location, rewrite equation 14 in terms of T_c and T_g . Thus, a window collected at $t = nT_c$ must be mapped to the time given by

$$t = \text{mod}(nT_c, T_g). \quad (17)$$

Let $g(t)$ be a sampling function with a period of T_g (see figure 6(b)). To map the window into the appropriate location, convolve the windowed signal with $g(t)$, yielding $[H_{j,0}x(t)u(t)v(t - nT_c)] * g(t)$, shown in figure 6(c). This is equivalent to the mapping performed in basic synchronous averaging, discussed in Section 2.2.3, with the period being the rotational period of the gear of interest. The primary difference is the application of the window in order to attenuate vibrations not associated with the gear under consideration. From equations 14 and 17, it is evident that in the initial state $n = 0$, the center of the period over which tooth $P_{0,g}$ meshes is mapped to $t = 0$, and each subsequent tooth is mapped appropriately. In addition, if $n_{Reset,g} = N_g$, then all of the teeth of the gear under consideration will be captured. In this case, once N_g windows have been mapped, a single synthesized vibration signal has been constructed.

In order to sufficiently extract a final time averaged vibration signal from the measured signal, a large number, M_e , of synthesized signals (or ensembles) must be captured and averaged. Thus, the final signal for the gear of interest is given by

$$X_g(t) = \frac{1}{M_e M_v} \sum_{n=0}^{M_e N_{Reset,g} - 1} [H_{j,0}x(t)u(t)v(t - nT_c)] * g(t). \quad (18)$$

2.3.3. Sun Gear Considerations

This methodology assumes that a window of data will be collected once per sensor per carrier revolution. However, for the sun gear case, data can be collected each time a planet passes the sensor, resulting in as many windows

per revolution per accelerometer as there are planet gears. Consider a planet gear tooth as it travels through a rotation of the planet gear. As the planet gear meshes with the ring gear, one face of the planet tooth contacts a ring gear tooth. As the planet gear meshes with the sun gear, the opposite face of the planet tooth contacts a sun gear tooth. Hence, damage on that face of a planet gear tooth could be interpreted as sun gear damage since it only appears when the planet meshes with the sun. This problem can be solved by collecting sun gear data during each planet passing, but separately analyzing each set of data associated with the passing of a given planet gear. The application of equation 18 using the sun gear parameters will yield this set of signals.

2.3.4. Single Transducer Limitations

The vibration separation technique was developed for use with a single transducer. However, the use of a single transducer leads to a number of limitations on its implementation.

The first limitation is whether the transmission geometry is appropriate to the methodology. As stated above, if the condition $n_{Reset,g} = N_g$ is met, then all of the teeth on the gear of interest can be captured. This condition will hold for the planet gears of most transmissions. However, this condition does not necessarily hold for the sun gear. Hence, even in a typical planetary transmission, the single transducer methodology may not be sufficient to capture all of the teeth of a sun gear. In addition, the methodology will not work in a non-typical transmission, where the condition does not hold for the planet gears.

The second limitation is the time required to obtain the final set of averaged vibration signals. If $M_v = 1$, i.e. the chosen window width is one tooth, and M_e ensembles are required, then the time required to obtain the final signal is $M_e N_g T_c$. In general, to sufficiently separate the desired vibration from the measured vibration, many ensembles are required.

The final limitation of the single transducer technique is a lack of robustness, which is manifested in two ways. First, if the transducer fails, then no vibration data can be collected and the health monitoring system will go offline. Less obvious, however, is that the use of a single transducer causes the system to be susceptible to corruption from any noise source whose period is commensurate with the period of rotation of the carrier. Since a single transducer collects data for a tooth of the gear of interest for only a single angular position of the carrier, then any external disturbance that is synchronized with the carrier and occurs at that carrier orientation will not be removed by averaging, but rather enhanced. This external disturbance could ultimately corrupt the averaged vibration signal, triggering a false alarm, or worse, masking a feature in the signal that would otherwise indicate damage.

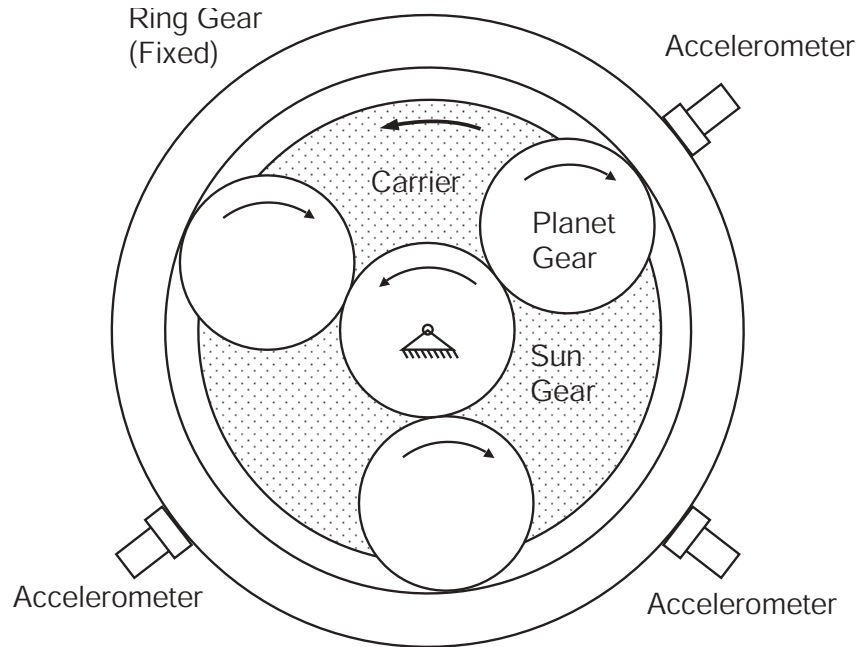


Figure 7. Multiple Transducers

2.4. Vibration Separation Generalized to Multiple Transducers

In order to overcome the limitations of the single transducer vibration separation technique, Samuel and Pines proposed the extension of the technique to the use of multiple transducers(3). The methodology presented by McFadden is generalized to include input from multiple transducers. However, the underlying theory of the multiple transducer technique is the same as that of the single transducer technique.

2.4.1. Theory

In order to extend the theory to the case where multiple transducers are mounted at various points around the ring gear (see figure 7), a second assumption must be made. *The multiple transducer extension of the vibration separation technique assumes that the vibration signals obtained from multiple transducers positioned about the ring gear are nominally similar.* Thus, the ring gear teeth near the transducers must all be free of damage, and the positions of the transducers relative to their respective teeth must be the same. If the assumption holds, then vibration data windows collected from all of the transducers can be mapped to generate a single averaged vibration signal. The applicability of this assumption is discussed below in section 2.4.3.

2.4.2. Methodology

First consider again a single accelerometer. Define the accelerometer as $j = 1$, and let it be radially aligned with the ring gear tooth $P_{j,r} = P_{1,r} = 1$. Recall that the transfer function between the accelerometer and the planet

gear $h_j(t)$ is defined such that the first peak of the function occurs at time $t = 0$. Letting this peak be associated with the point that gear tooth $P_{0,g} = 1$ is aligned with ring tooth $P_{1,r} = 1$, $h_j(t) = h_1(t)$. This condition defines the state of the gearbox at $n = 0$ for accelerometer 1.

Next, consider a second accelerometer aligned with ring tooth $P_{2,r}$, numbered sequentially from ring tooth 1 in the direction of carrier rotation. Define the spacing between two accelerometers j and 1, in terms of the number of ring teeth, as

$$S_{j-1} = P_{j,r} - P_{1,r}. \quad (19)$$

Hence, the spacing between accelerometers 1 and 2 is given by

$$S_{2-1} = P_{2,r} - P_{1,r} = P_{2,r} - 1. \quad (20)$$

Recall that at time $t = 0$, the gear under consideration is passing accelerometer 1 and gear tooth $P_{0,g} = 1$ is aligned with ring tooth $P_{1,r} = 1$. Thus, after S_{2-1} tooth mesh periods, at time $t = T_m S_{2-1}$, the gear under consideration will pass accelerometer 2. At this state, gear tooth $P_{0,g} + S_{2-1}$ will mesh with ring tooth $P_{2,r}$. As a consequence of shifting the second sensor S_{2-1} teeth around the ring gear, a time shift is introduced into the transfer function between accelerometer 2 and the planet gear, $h_2(t)$. Hence, the first peak of $h_2(t)$ occurs at time $t = T_m S_{2-1}$, and subsequent peaks occur at $nT_c + T_m S_{2-1}$. This condition defines the state of the gearbox at $n = 0$ for accelerometer 2.

To accommodate the shift in $h_2(t)$, the windowing function for accelerometer 2 must be shifted by $t = T_m S_{2-1}$ yielding $v_2(t - (nT_c + T_m S_{2-1}))$. Thus, the final synthesized signal for the gear of interest using accelerometer 2 is $[H_{2,0}x(t)u(t)v(t - (nT_c + T_m S_{2-1}))]_2 * g(t)$. Assuming that the levels of vibration measured by all sensors are nominally equal, $H_{j,0} = H_0$. Thus, for a general accelerometer j , the synthesized signal is $[H_0x(t)u(t)v(t - (nT_c + T_m S_{j-1}))]_j * g(t)$. As validation, it can be seen that for a single sensor $j = 1$, $S_{1-1} = 0$ and the above statement simplifies to $[H_0x(t)u(t)v(t - nT_c)]_1 * g(t)$. It should be noted that even though the window function is shifted in time, the convolution ensures that a signal synthesized from a given sensor is correctly phased with a signal synthesized from any other sensor.

Finally, the measured vibrations from J sensors are incorporated into the final averaged signal $X_g(t)$, using

$$X_g(t) = \frac{1}{M_e M_v J} \sum_{n=0}^{M_e N_n \text{Reset}, g - 1} \sum_{j=1}^J [H_0x(t)u(t)v(t - (nT_c + T_m S_{j-1}))]_j * g(t) \quad (21)$$

In this case, the number of ensembles used to obtain $X_g(t)$ is $M_e J$. Recall that the time required to collect M_e ensembles with one sensor is $M_e N_g T_c$. In this same time period, using multiple sensors, $M_e J$ ensembles are collected. Thus, to collect M_e ensembles using J sensors, a time period of $(M_e/J)N_r T_c$ is required. Note that

M_e must be divisible by J . For two accelerometers, the time required to obtain a final set of vibration data is half that required when using one accelerometer.

An additional benefit of using multiple sensors is the ability to collect data from teeth not seen by a single sensor. This situation occurs when $N_g > n_{Reset,g}$. The number of sensors required to capture an entire gear is $J = \lceil N_g/n_{Reset,g} \rceil$. If these sensors are placed around the ring gear such that each sensor captures a tooth not captured by any other sensor, then all the teeth of the gear of interest will be captured.

Possibly the greatest benefit of using multiple transducers is significantly increased robustness to both sensor failures and synchronized noise. First, if a sensor failure is detected, the algorithm can be easily adapted to capture data from the remaining sensors. This will result in an increase in the time required to capture a final vibration signal, however, the health monitoring system will remain online. Second, as stated above, a single transducer is susceptible to any external disturbance whose period is commensurate with the period of rotation of the carrier and occurs during a carrier state where data is collected. However, since the use of multiple transducers allows data to be collected during multiple carrier orientations, synchronized noise can be eliminated by the averaging process.

2.4.3. Multiple Transducer Limitations

The primary limitation of the multiple transducer vibration separation technique stems from the underlying assumption that the vibration signals measured by the transducers are nominally similar. A simple study of the vibration signal waveform generated by a single tooth mesh was conducted using the University of Maryland Transmission Test Rig (UMTTR). The sensitivity of the waveform to various factors such as damage and sensor location was investigated.

As part of this study, the similarity of vibration signals collected from accelerometers mounted about the ring gear of a planetary transmission was examined. Four accelerometers were placed on the ring gear in a highly controlled fashion. Vibration signals were collected from each accelerometer and the single transducer vibration separation technique was used to process them. A Tukey window (discussed in the following section) was used with the vibration separation algorithm, and 25 ensemble averages were performed to yield each separated signal. Figure 8 shows a single tooth mesh period corresponding to tooth five of planet gear two as seen by each accelerometer. Note that the transmission under consideration has a contact ratio of 1.2. Thus, the tooth is undergoing mesh for a period of $1.2T_m$, and the x-axis of the figure is labelled to reflect this fact. Certain features of the signals are seen to compare favorably, e.g. the peaks at -0.08, 0.81 and 0.96. However, the differences are significant, most notably in the range from 0.1 to 0.6. For example, consider the signal around 0.37. Accelerometers 1 and 2 both peak at this point, although the peaks are of different shapes. However,

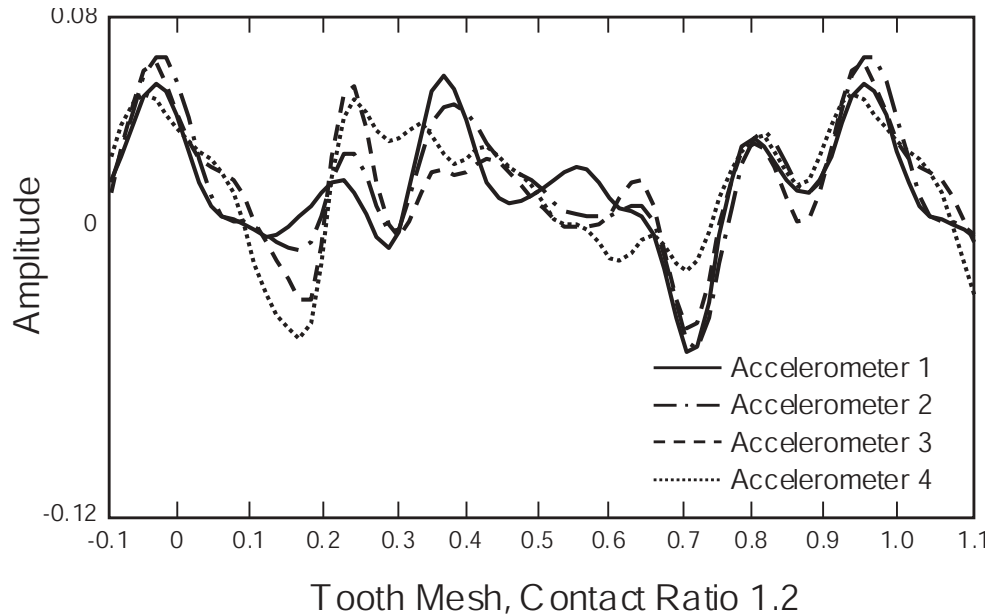


Figure 8. Tooth Mesh Waveforms from Four Accelerometers: Planet 2, Tooth 5

accelerometers 3 and 4 both have valleys at this point, though once again, the valleys are significantly different in shape. Thus an average of the signals would not be meaningful or useful. It should also be noted that at present, the accelerometer position can be controlled to a much higher degree in the laboratory environment than in an actual rotorcraft transmission. Thus, the multiple transducer assumption does not currently hold, and as a result, the technique is not used in this research. However, research into the development of new sensor technologies is continuing, and it is expected that the technique will eventually prove useful.

2.5. Window Selection and the “Australian Patent” Technique

When implementing the vibration separation algorithm, a window function must be selected. In the development above, a rectangular window was assumed for simplicity. However, any number of windows may be used as long as certain conditions are satisfied.

2.5.1. Conditions on the Window Function

McFadden stated that two conditions must be satisfied by the desired window function(2). First, the minimum window width required to produce a valid synthesized vibration signal is one tooth mesh period, T_m . Second, the shape of the window must be chosen such that when all the windows necessary to construct a single synthesized signal are mapped to their appropriate locations, the sum of the windows must be constant. This is necessary to ensure that no artificial amplitude modulation results as an artifact of the procedure.

If $n_{Reset,g} = N_g$, then the simplest window that satisfies these conditions is a rectangular window with a width of one tooth mesh period, T_m , i.e. $M_v = 1$. Note that if $n_{Reset,g} < N_g$, then the window width can be increased to satisfy the conditions.

However, simply satisfying the conditions for a valid synthesized signal is not necessarily sufficient for the selection of an appropriate window. The choice of window has an effect on the resulting shape of the vibration signal. Thus, a comparison of the properties of various window functions is required.

2.5.2. Additional Window Function Considerations

After satisfying the conditions necessary for the selection of a valid window, two parameters may be adjusted: the window width and the window shape.

Recall the primary assumption underlying vibration separation, that when a given planet gear is near a transducer, the vibrations measured by the transducer are dominated by the meshing of that specific planet gear with the sun and ring gears. Conversely, when the planet is further from the transducer, the contribution of that specific planet gear is reduced, and thus the contribution of other excitation sources may be more prevalent. In addition, when the planet of interest is at the transducer, the contribution of the other planets relative to the planet of interest is at a minimum. However, when the planet of interest is approaching or receding from the transducer, then the contribution of the previous or following planet, respectively, is increased. Since each planet has the same number of teeth and the same rotational frequency, each planet other than the planet of interest constitutes a vibration source with a period commensurate with the period of interest, and thus the vibration is not attenuated by the averaging process. Hence, a small window width is desired.

Once again, the simplest window that fulfills the above desired property is a rectangular window with a width of $M_v = 1$. However, the rectangular window introduces additional problems. Specifically, a rectangular window can introduce small discontinuities where the windows meet. This problem can be attenuated by the use of a window function with smooth, antisymmetric shoulders such as a triangular, Hanning or raised cosine bell window. In each of these cases, the windows will overlap. However, the sum of the windows required to assemble a single synthesized signal will remain constant.

Two important factors should be considered when using a window width greater than T_m , i.e. $M_v > 1$. First, it must be recognized that the signal collected prior to and subsequent to the primary tooth mesh waveform of interest are associated with a planet tooth meshing with a different ring tooth than the one nearest the transducer. In addition, these waveforms may be slightly distorted, as the planet is not at the minimum distance from the transducer when they are collected. Thus the use of a wide window is a trade off between distortions due

to window junctions, and distortions due to planet/transducer proximity differences. Second, the windows near the edges of the synthesized signal will tend to extend beyond the edges of the signal and thus the synthesized signal will have a period greater than desired. The desired signal should exist only for $0 \leq t < T_g$. Since the synthesized signal is assumed to be periodic, this problem can be corrected by mapping the windows on a circle. This can be thought of as truncating the signal outside the desired range, then summing any portion of the signal which existed for $t < 0$ with the end of the truncated signal, and summing any portion of the signal which existed for $t \geq T_g$ with the beginning of the truncated signal.

McFadden presented a comparison of the spectra of a narrow, rectangular window with $M_v = 3$, a wide rectangular window with $M_v = 6$, a triangular window with $M_v = 6$, and a Hanning window with $M_v = 6$ (29). Through numerical and experimental comparisons, it was concluded that the Hanning window would yield the smallest errors.

However, given that the Hanning window does not have a flat top, the tooth mesh waveform of interest may be distorted. Thus the use of a Tukey window is proposed. The Tukey window(30) is a flat-top Hanning window, and the coefficients for a discrete time, N point window is given by

$$w[k+1] = \begin{cases} 1.0 & \text{for } 0 \leq \|k\| \leq \frac{N}{2}(1+\alpha) \\ 0.5 \left[1.0 + \cos \left[\pi \frac{k - \frac{N}{2}(1+\alpha)}{N(1-\alpha)} \right] \right] & \text{for } \frac{N}{2}1 + \alpha \leq \|k\| \leq N \end{cases} \quad (22)$$

where the taper ratio α defines the fraction of the total window width encompassed by the shoulders. A Tukey window with $M_v = 5$ and $\alpha = 0.8$ would leave the primary tooth mesh waveform of interest unaffected while providing smooth shoulders. The various window shapes are shown in figure 9.

2.5.3. The “Australian Patent” Technique

In the mid 1990’s, Forrester developed a technique for extracting the time averaged vibration signals associated with the individual planet gears in a planetary gearbox from a composite vibration signal(25). In 1994, an Australian patent was obtained for this technique(31), informally referred to as the “Australian Patent” technique. A United States provisional patent was subsequently obtained in 1998(32). It was later extended to the extraction of sun gear vibration signals(26).

Although the mathematical development of the technique presented by Forrester is somewhat different than that presented by McFadden(2), the resulting windowing/mapping algorithm is the same in each case. The only unique aspect of Forrester’s work is the placement of a third condition on the window function. Forrester stated that there should be no loss of data in the windowing process, in contrast to McFadden, who suggested the use of a narrow window causing much of the data between planet lobes to be discarded. Thus, Forrester placed a

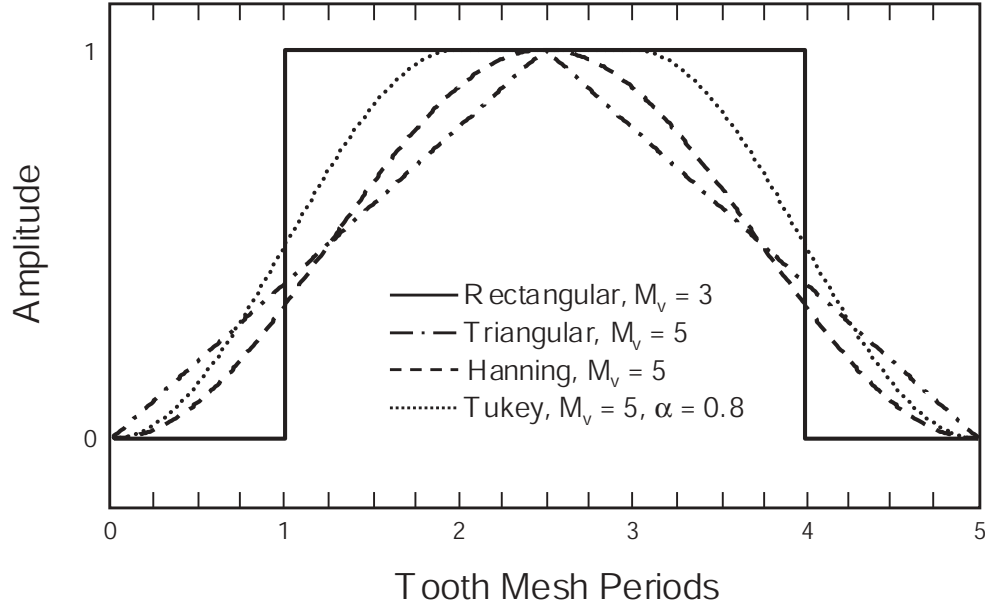


Figure 9. Comparison of Various Window Functions

condition on the window function that the summation of the windows used for each planet should be a constant, ensuring that the sum of the individual planet averages would be proportional to the sum of the total vibration, i.e. no loss of data. The window proposed by Forrester, herein referred to as the Forrester window, applied to planet p in a transmission with P planets is given by

$$w_p(t) = \left(a \left(1 - \cos \left(2\pi f_c t - \frac{p2\pi}{P} \right) \right) \right)^{P-1} \quad (23)$$

Forrester reported an improvement in the performance of damage detection techniques when applied to vibration data separated using his window rather than a narrow one. However, the use of a wide window such as his may result in significant distortions in the individual tooth mesh waveform. Thus, a comparison of tooth mesh waveforms as produced by various windows is required.

2.5.4. Comparison of Window Functions

A comparison of individual tooth mesh waveforms produced by various windows is presented. Figures 10-14 show the waveforms associated with planet 2, tooth 5 (chosen arbitrarily) operating under no-damage conditions. Figures 15-19 show the waveforms associated with planet 2, tooth 5 where all teeth on planet 2 are spalled.

Specifically, a narrow, rectangular window with $M_v = 3$, a wide rectangular window with $M_v = 6$, a triangular window with $M_v = 6$, a Hanning window with $M_v = 6$, a Tukey window with $M_v = 5, \alpha = 0.8$ and Forrester's window for a three planet transmission are compared. Again, the transmission under consideration has a contact ratio of 1.2, and the figures are labelled accordingly. The waveform produced using the narrow

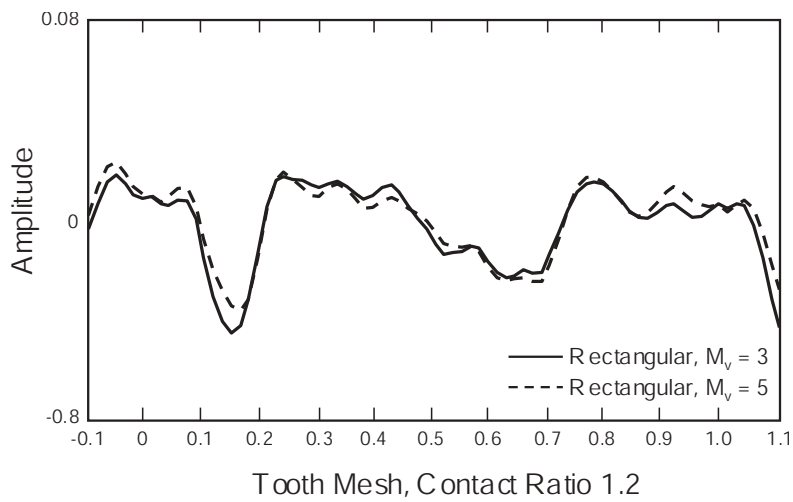


Figure 10. No-Damage Condition Tooth Mesh Waveforms Generated Using Narrow Rectangular and Wide Rectangular Windows: Planet 2, Tooth 5

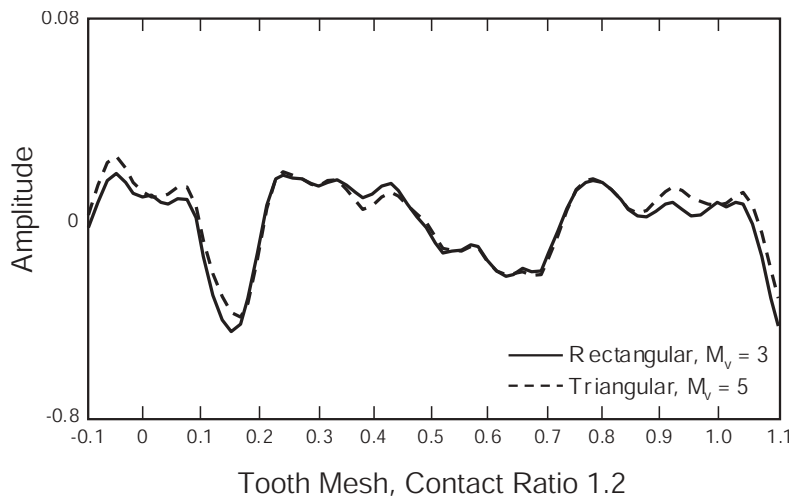


Figure 11. No-Damage Condition Tooth Mesh Waveforms Generated Using Narrow Rectangular and Triangular Windows: Planet 2, Tooth 5

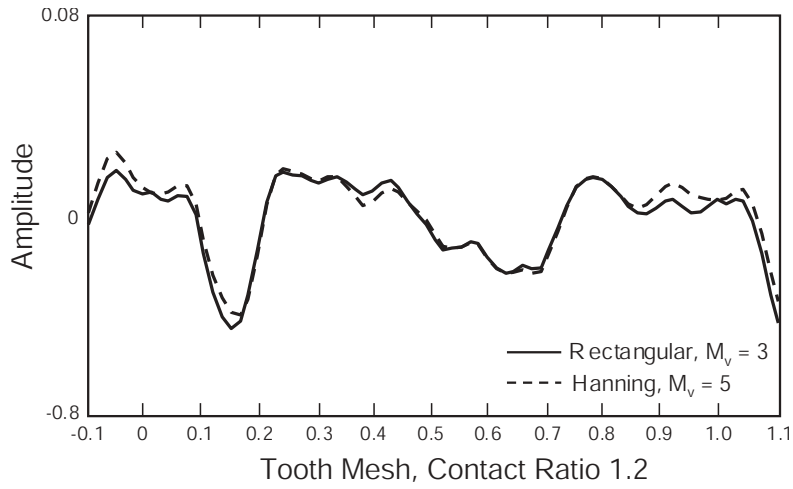


Figure 12. No-Damage Condition Tooth Mesh Waveforms Generated Using Narrow Rectangular and Hanning Windows:
Planet 2, Tooth 5

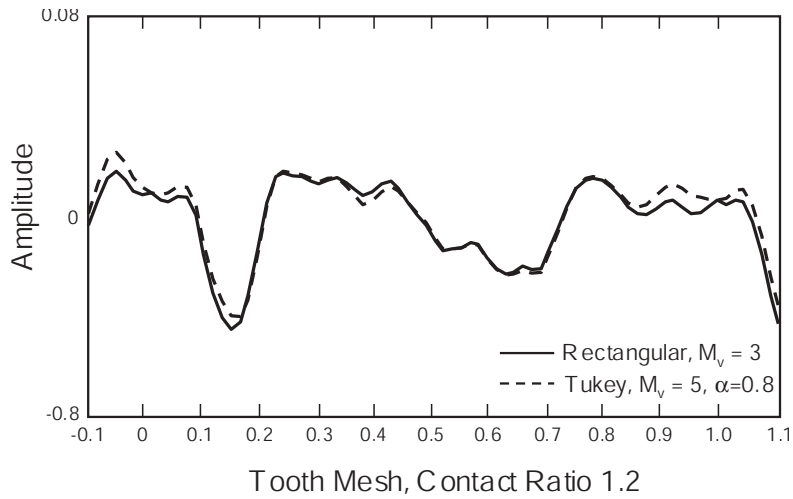


Figure 13. No-Damage Condition Tooth Mesh Waveforms Generated Using Narrow Rectangular and Tukey Windows:
Planet 2, Tooth 5

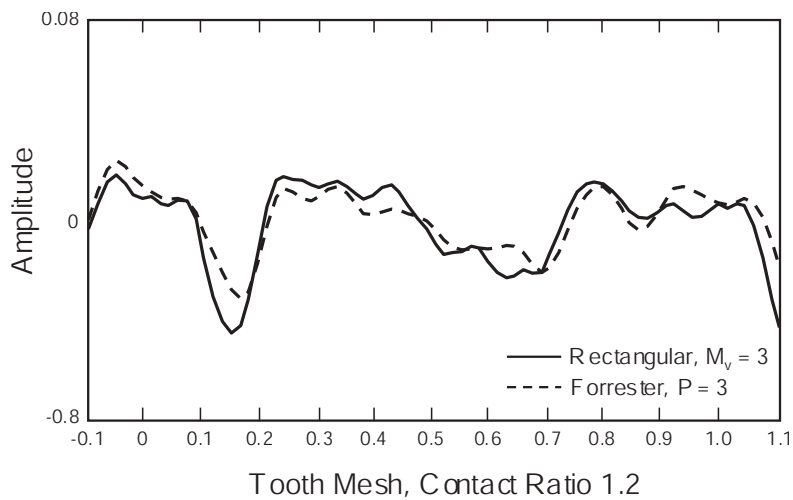


Figure 14. No-Damage Condition Tooth Mesh Waveforms Generated Using Narrow Rectangular and Forrester Windows: Planet 2, Tooth 5

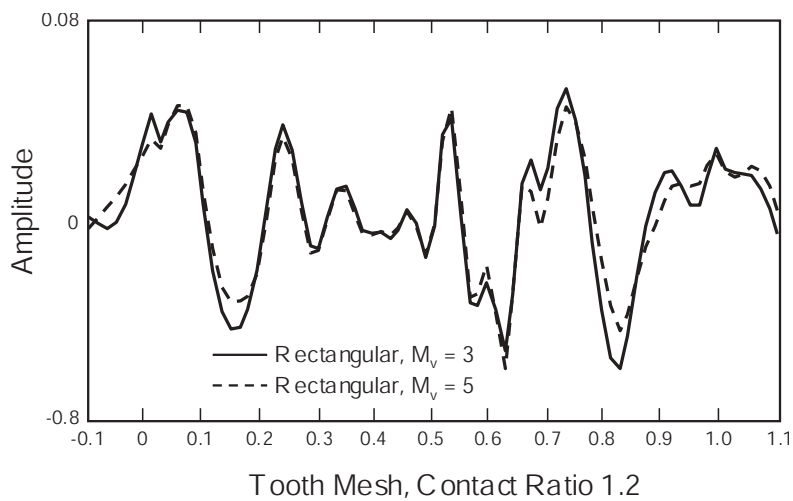


Figure 15. Damage Condition Tooth Mesh Waveforms Generated Using Narrow Rectangular and Wide Rectangular Windows: Planet 2, Tooth 5

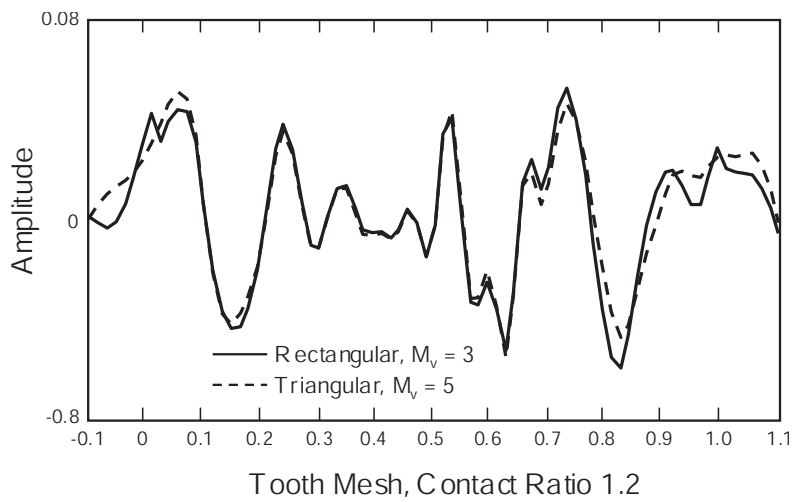


Figure 16. Damage Condition Tooth Mesh Waveforms Generated Using Narrow Rectangular and Triangular Windows:
Planet 2, Tooth 5

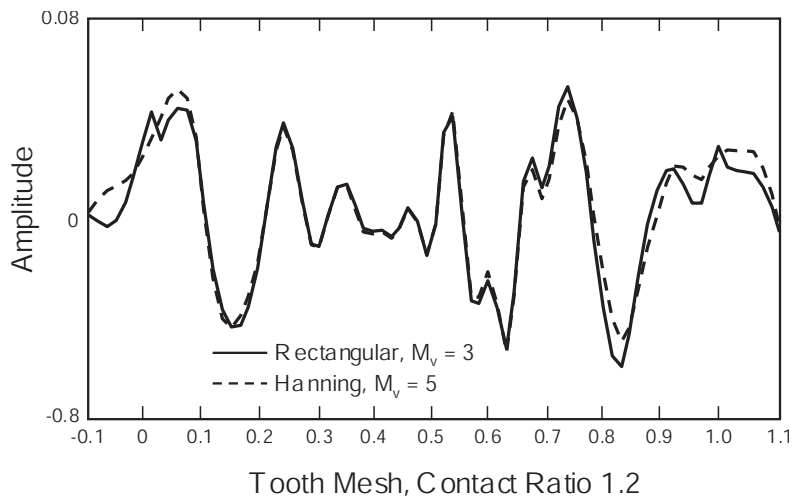


Figure 17. Damage Condition Tooth Mesh Waveforms Generated Using Narrow Rectangular and Hanning Windows:
Planet 2, Tooth 5

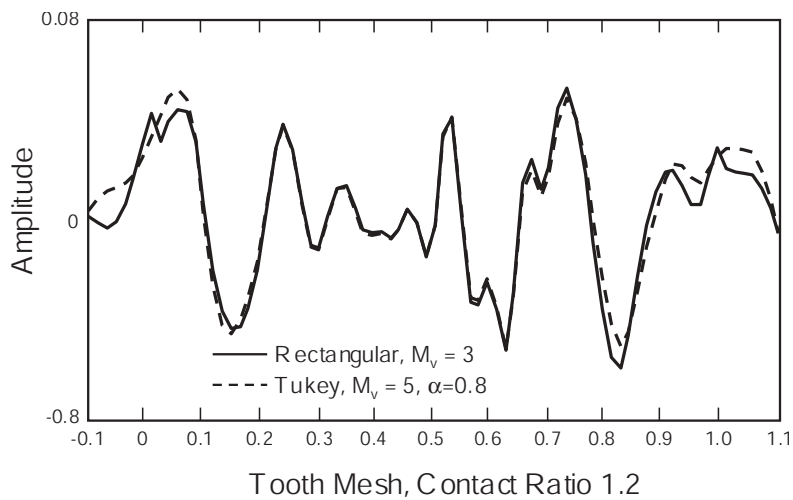


Figure 18. Damage Condition Tooth Mesh Waveforms Generated Using Narrow Rectangular and Tukey Windows: Planet 2, Tooth 5

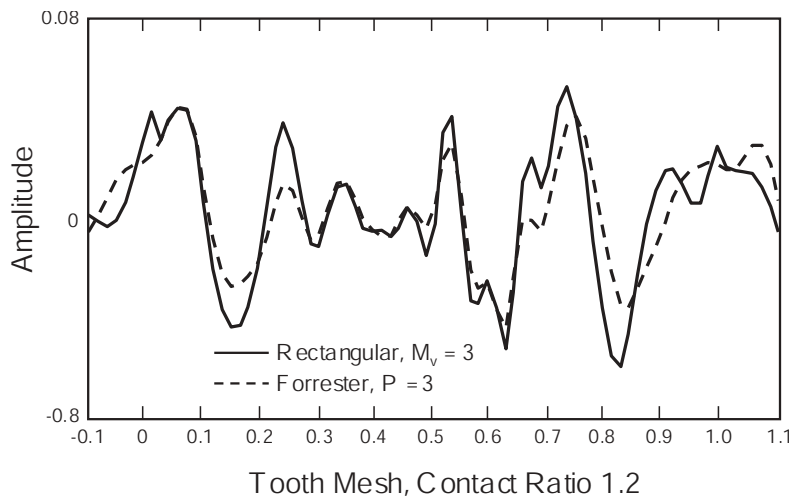


Figure 19. Damage Condition Tooth Mesh Waveforms Generated Using Narrow Rectangular and Forrester Windows: Planet 2, Tooth 5

rectangular window is taken as a baseline of comparison as it is expected to yield minimal distortions in the shape of the waveform.

First, consider the use of a rectangular window as shown in figures 10 and 15. Since the contact ratio is 1.2, the actual mesh period is greater than T_m , specifically $1.2T_m$. However, the windows are mapped and assembled using T_m as the tooth mesh period. Thus, the windows meet at the points in the tooth mesh waveform labelled 0 and 1. An inspection of these points reveals the presence of a small peak. This peak is most prevalent in figure 15 at point 0. However, it is present at each window meeting point for each rectangular window, though the wider rectangular window attenuates the peak to some extent. However, an inspection of the remaining figures shows all the windows in this study with smooth shoulders completely attenuate the peak, thus effectively eliminating the small discontinuities caused by the assembly process. Hence a window with smooth shoulders is preferable.

However, with the exception of the locations where the windows meet, the rectangular window is expected to produce the most accurate waveform. Thus, the desired window is the one which produces a waveform closest to that of the rectangular window, while still possessing smooth shoulders. First consider the no-damage condition. From an inspection of figures 10-14, it can be seen that the window which best fulfills this requirement is the Tukey window. This is most evident in the peaks at 0.16 and 0.43. Next consider the damage case. From an inspection of figures 15-19, it is again evident that the Tukey window best fulfills the requirement. This can be seen by inspecting the majority of the peaks, e.g. the peaks at 0.16, 0.54, 0.63 and 0.73. It should be noted that the Forrester window produces a waveform significantly different from the baseline as shown in figures 14 and 19.

Given these results, the Tukey window is used for the remainder of this research. The next section describes the real-time software developed for the implementation of the vibration separation algorithm.



Figure 20. Hardware Setup.

3. REAL-TIME VIBRATION SEPARATION USING LabVIEW™

3.1. Introduction

With an improved ability to separate planetary gear vibration signatures, the development of new and better algorithms to detect planetary gear damage can be supported by a testbed that is reliable, convenient, and easy to use. The goal of this program is to establish a baseline to allow for standardized comparisons of diagnostic algorithm outputs which would enhance research consistency and help to obtain results quicker(33).

This software package is based on an extension of McFadden’s technique which accommodates processing of vibration signals from up to 4 sensors simultaneously. With this software package, a user can integrate a new diagnostic algorithm to accompany the existing algorithms, allow the program to perform the multi-sensor modified technique of vibration separation, and focus solely on the desired diagnostic output results, displayed in real-time. By knowing the geometry of the gearbox, and supplying counter pulses that demarcate individual revolutions of the gearbox, (one pulse every revolution and a gear-to-carrier reset trigger), a user can continually receive output vectors of all the teeth in the planets and sun as they are assembled. The number of times the gear system must rotate to assemble a planet vector for a transmission with a hunting tooth ratio between the planets and ring gear, and the sun and ring gear, is equal to the number of planet teeth. For this program, the position of the sun gear in relation to the planet gears, including all of the teeth, is assumed to reset every (*sun gear teeth*) \times (*planet teeth*) rotations of the gear system.

These organized vectors are then available to be processed with a diagnostic algorithm. This LabVIEW-based(34) real-time program has been designed to be as modular as possible to allow for upgrading and altering to suit particular project requirements. This modularity allows new algorithms to be quickly and efficiently integrated into the program in addition to the standard included stationary metrics FM4 and NA4. Finally, the data from the program and metrics is easily and conveniently saved to files that can be later imported into an external application, or just saved as a record of the acquisition. With this software package, it is possible to receive data from up to 4 accelerometer sensors from a planetary gearbox that contains up to 4 possibly



Figure 21. UMD LabVIEW™ Diagnostic System.

non-equidistant planets. In order to maximize portability for field testing, the hardware for the system was selected for minimum size while not compromising on computing power. The laptop computer has the power of a desktop with its 2 GHz processor, 512 MB of RAM, and 32 MB ATI graphics card. An additional battery allows a user to operate away from a wall power source for extended periods of time. The data acquisition system uses a National Instruments DAQCard-6062E, a PCMCIA card. The NI BNC-2120 BNC connector block is also small in size. These components combine to form a system that can be easily stored and transported. Figure 20 shows where each component fits into the system, and figure 21 shows the actual system.

3.2. Data Handling

The program requires a nominal number of required inputs from the user to run. The program uses the number of planet, sun, and ring teeth to find the planet and sun vectors that describe the progression of teeth from revolution to revolution. The indices marking the center of the planet lobes in the revolution waveforms are found using the sensor spacing relative to the planets at the time the 1/rev counter pulses. The required input fields for an acquisition are shown in figure 22 along with typical values. The device number is a LabVIEW specific input, generally equal to one. The *channels* input specifies the 1/rev pulse and the 4 sensor inputs. The Ring, Sun, and Planet Teeth inputs are the number of teeth for each component. The *mesh period in scans* input specifies the number of samples desired for each tooth. The *mesh window* input specifies how wide in teeth the data segments should be. Changing the *Scan Rate* changes how fast the hardware samples the sensors. Finally, the *Sensor and Planet Input Parameters* input specifies the position of the planets, in radians, in relation to the sensors at the time of the 1/rev pulse.

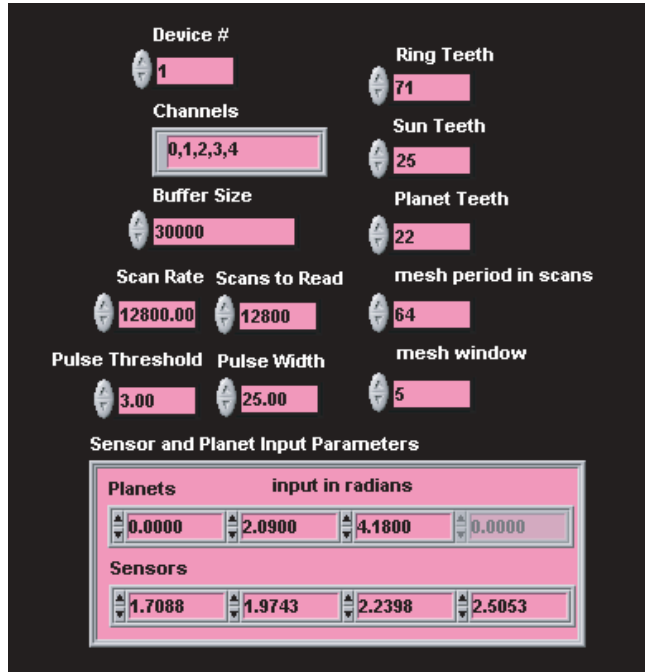


Figure 22. Necessary Program Inputs.

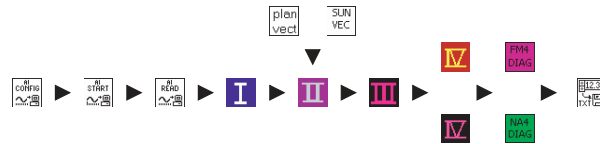


Figure 23. Program Flow.

The hardware inputs required for a typical acquisition include a gear to carrier reset pulse train, a once per rev pulse train, and up to 4 accelerometer sensors to detect the vibrations in the ring. The Primary Tooth Vector Assembly Loop is contained within a loop. The purpose of the Primary Tooth Vector Assembly Loop is to obtain $(sensors) \times (planets)$ 1-D vectors that are $(planet\ teeth) \times (samples\ per\ tooth)$ in length. These teeth vectors, available for both the planets and the sun with respect to each of the planets, display each tooth averaged a number of times input by the user. This is usually set to be the number of sun teeth. The weighted average occurs as each Planet Vector is assembled. Each sensor extracts only one tooth every time the system rotates. Thus, by dividing the number of planet teeth by the rotational frequency of the system, the time it takes to produce one tooth vector average can be found where each tooth vector is comprised of $(planet\ teeth)$ of teeth windows placed overlapping each other.

Figure 23 shows the major VI functions within the program. Each block represents a subVI function in the

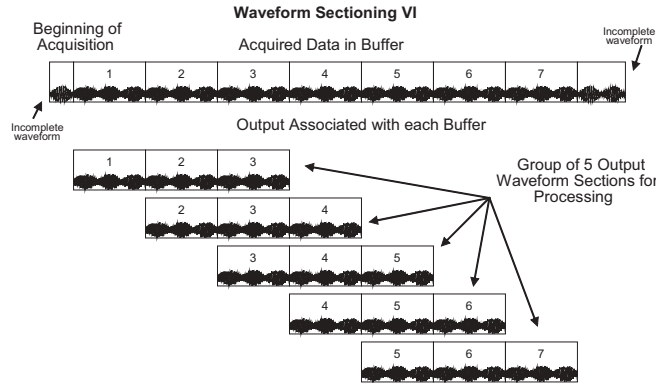


Figure 24. Sectioning of Revolution Waveforms.

program. The blocks labeled with numbers are, chronologically: The Waveform Sectioning VI, The Selection and Cropping VI, The Windowing and Assembly VI, and the two Averaging VIs, (one for the planets and one for the sun). The NA4 and FM4 blocks are diagnostics, and the last block is the Save to File function. The configuration of the National Instruments DAQ hardware must occur first. Before any data is collected the necessary hardware input parameters such as the trigger channel and level are input to the library functions A.I. Config and A.I. Start. A.I. Start receives a command to begin a continuous acquisition that acquires and stores data from the 1/rev counter pulse train and all the accelerometers into the hardware buffer. Every rotation of the system, a given sensor will see a different tooth on a given planet from the tooth seen in the previous rotation. Because the progression of teeth is almost never chronological, a vector must be calculated to describe this progression. The vectors computed for the planets and sun are input into the Selection and Cropping VI and used to assign tooth numbers to the data segments produced there. The program loop that contains all of the subVI functions necessary to produce one set of planet and sun output vectors is dubbed the Primary Tooth Vector Assembly Loop. All of the VIs in figure 23 are inside this loop with the exception of the AI Control, AI Start, and Save File Functions.

3.3. The Waveform Sectioning VI

The data output from the AI Read VI is in the format of a 2D matrix. The matrix contains a number of columns specified by the number of total software inputs. This includes the 1/rev trigger and the number of sensors. This data matrix then needs to be appropriately divided into individual waveforms that represent one revolution each. The 1/rev trigger is used to provide the markers for sectioning. A potential problem arises if the planet lobe that will be examined is too close to one of the sensors at the time of the 1/rev pulse. The data segment window is the window, usually multiple teeth long, that is placed astride the planet lobe to designate that area to be cropped and sent to the next VI. The problem arises if a portion of the data segment window lies outside of the

boundary demarcated by the 1/rev trigger. To allow for a simple and robust design to the program, the solution involves concatenating the revolutions that were temporally before and after the central revolution waveform to their respective locations in the vector. If a window falls outside of the central boundary, the window can access the data from the buffers before and/or after.

To implement this process, the indices of the pulses from the 1/rev trigger are used to find the next 3 full revolution waveforms and branch them off for processing. The program then crops off only the next one revolution waveform and deletes it. By continually reading the next three waveforms and cropping off only the first waveform, the output will be vectors that each contain 3 revolution waveforms with middle waveform always the waveform that will have the processing operations applied to it while the flanking waveforms provide a kind of temporal buffer to allow for data segment windows that may overrun the width of the current middle revolution undergoing processing. Figure 24 graphically describes the process that is occurring in this sub VI. Each of the output revolutions has been interpolated in the subVI to be the mesh period in scans times the number of ring teeth, both inputs, for each revolution. Therefore, each output waveform section will be three times this number. Because of this interpolation, the analysis may move out of the time domain and into the positional domain and the mesh frequency and harmonics are found to be the number of planet teeth and multiples of the number of planet teeth respectively. The number of final output waveforms of the Waveform Sectioning VI produced each iteration depends on the frequency of the gearbox and the settings for scan rate versus scans to read. Except for the first iteration, with these two settings the same, the number of outputs will be the floor of the frequency. For example, a rotational speed of 5.25 Hz. will result in 3 iterations of 5 waveforms followed by an iteration with 6 waveforms as this iteration buffer includes not only 5.25 revolutions itself, but also .75 revolutions from the three previous buffers that have been concatenated each time, resulting in an output of 6 waveform sections on that iteration.

3.4. The Selection and Cropping VI

The output of the Waveform Section VI is input into the select and crop VI. This input is a 2D matrix of rows equal to the number of waveform sections and columns equal to 3 times the number of ring teeth multiplied by the mesh period. Using the geometry of the gearbox and sensors when the 1/rev channel pulses, the locations of the centers of the planet lobes in the revolution waveform are calculated. With the resulting indices from this calculation, the program takes each waveform section in turn and crops out the data segments where the planet is passing the sensor. The width of these data segment windows is user defined in units of teeth on the front panel. The number of data segments for each sensor will be equal to the number of planets in the system. The output from this VI is a cluster containing 4 planet matrices, even if 4 planets have not been specified. Each

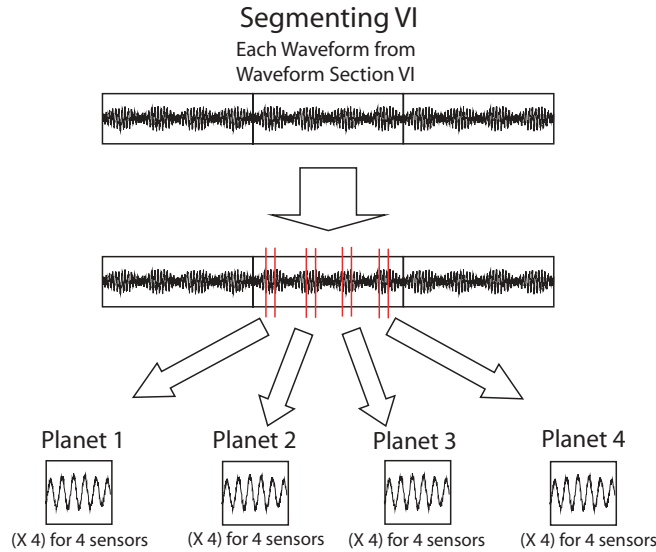


Figure 25. Extraction of Data Segments from Individual Revolution Waveform.

planet matrix is a 3D matrix where each page is one iteration or one revolution, each row is a sensor and the columns are the data. The data length will be the product of the mesh period with the mesh window. The number of iterations will be equal to the number of revolution waveforms that came into the VI. Figure 25 explains graphically the flow and distribution of the data through the selection and crop VI. Each output data segment is assigned a planet number using the input mesh order vector. Once the first element of the mesh order vector is concatenated with the produced data segments from each waveform section, the first element of the vector is rotated to the end of the vector to allow the next incoming data to be assigned the next value in line. The sun vector is used in a similar way to assign tooth numbers to sun data segments.

3.5. The Windowing and Assembly VI

The data is input as it was output from Selection and Cropping VI. The data segments, each of which assigned a tooth number that it is centered on, are now windowed and mapped to their respective locations to create tooth vectors. The final output planet vectors are assembled in the order of tooth number using the concatenated tooth values., With data segments that are pulled from 4 different sensors and 4 different planets, there are a total of 16 different tooth vectors to assemble from these data segments. The windowing process involves multiplying each of the data segments by a window, as seen in figure 28 and figure 26. The purpose of this process is to emphasize the signal at the tooth under consideration without neglecting surrounding vibrations. LabVIEW comes with many standard windows that can be integrated, but by default the diagnostic software includes the Tukey window in figure 26 defined by equation 22.

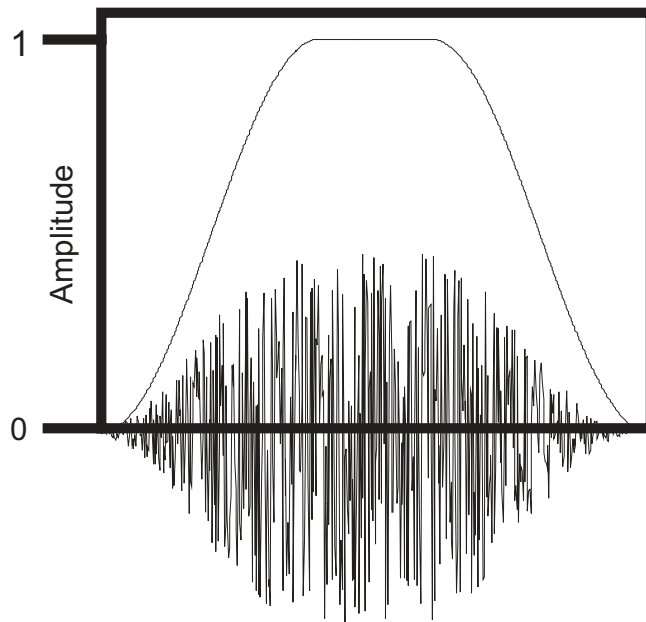


Figure 26. Window Applied to Tooth Vibration Signatures.

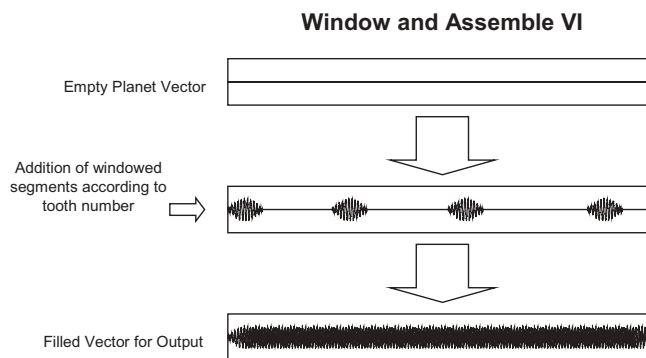


Figure 27. Windowing and Assembly.

For a mesh window width greater than one tooth, overlap will occur. The decaying edges of the window are designed to compensate for the increase in amplitude due to the addition of overlapping sections. The windowing function also re-centers the windowed data segments about zero using the mean value of the data segment. The data segments are read into the main loop of this sub-VI. The tooth numbers that were concatenated to the data segments are removed and used to define the appropriate location in the tooth vector for the windowed data segment. Once these tooth vectors are filled, they are exported and new initialized vectors of zeros are begun.

3.6. Average VI

The exported teeth vectors for each planet/sensor combination are input into Average VI. Each incoming planet and sun tooth vector is averaged with the previous associated vectors using this equation: $((x) * previous + new)/(x + 1)$ where x is the number of previous iterations, and previous and new are the vectors. The only purpose of this VI is to keep track of the previous averages in a software buffer so they can be averaged with the new updated teeth vectors.

3.7. Final Output

There are 32 output vectors for every iteration of the Primary Vector Assembly Loop. This includes 16 vectors for the planets and 16 for the sun as seen through the planets. Should a total of 4 planets and 4 sensors not be input into the front panel, there will still be 16 and the nonexistent planet/sensor combinations will be represented with vectors of all zeros. When these are saved to file, these zeros act as place holders to allow for easier import later on. The averaged teeth vectors are output to the windows on the front panel. In addition, they are saved for offline diagnostic processing. The included diagnostics FM4 and NA4 operate on these output teeth vectors. Only one value is calculated for each planet/sensor combination for each diagnostic. In order to obtain more averaged teeth vectors to calculate more diagnostic values, the Primary Teeth Vector Loop needs to iterate multiple times. The option is available on the front panel to allow for any number of Primary Teeth Vector Loop repetitions and hence any number of diagnostic calculations. Multiple numbers of diagnostic calculations over time have the potential to extend the use from diagnosis to prognosis. Figure 29 shows a typical output vector that includes vibration signatures from 22 teeth. In addition, several non-essential outputs are displayed through the front panel to help the user to monitor the data at each stage of the computing. Figure 28 shows these outputs. The top window shows a running average of all of the carrier revolutions. The middle window shows the raw data as it is stored in the buffer. The last two bottom windows display a sample of the data segments immediately before the windowing procedure and immediately afterwards. These outputs are not saved and are used primarily for aesthetic and debugging purposes. The output diagnostics are also saved to a file.

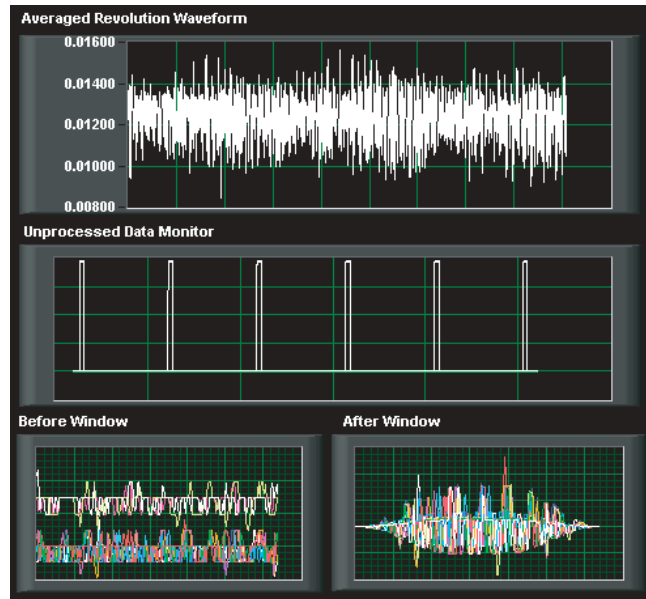


Figure 28. Non-Essential Outputs.

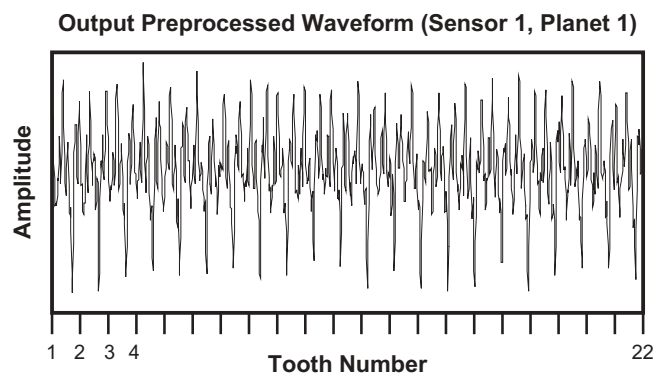


Figure 29. Output Planet Vector.

3.8. Included Diagnostics

The diagnostics are designed to be as modular as possible. Currently, two stationary diagnostics have been implemented, NA4 and FM4. Future work will involve implementing an adaptive lifting algorithm(35; 36), and a normalized energy metric(13), both developed at the University of Maryland. NA4 and other diagnostics require a running average of one of the outputs. In this case, a minimal additional amount of coding outside the diagnostic block is required to set up a software buffer to hold the running average.

The next section will discuss the constrained adaptive lifting diagnostic algorithm.

4. CONSTRAINED ADAPTIVE LIFTING DIAGNOSTICS

4.1. Introduction

In the ideal case, a mechanistic model of the transmission would be used to generate expected vibration signals for various cases to provide a basis for comparison. This approach, though, is still in the early stages of development(15). The advent of adaptive representations offers the potential to analyze a given vibration signal using a set of wavelet basis functions chosen from a set of fundamental wavelet bases that best represent the signal at each point. Hence, instead of using the wavelet transform solely to investigate changes in the characteristics of the vibration signal, a set of wavelets can be chosen to best fit a signal of a known operating condition, and then compared to the signal obtained from the transmission during use(14).

In order to effectively generate a model of transmission vibration signals that exist in the time domain, a method to implement the wavelet transform in the time domain is desired. One such method is the lifting scheme (16), a time domain prediction-error realization of the wavelet transform. Methods for adding adaptivity to the lifting scheme have begun to be investigated(17; 18). The method used in this work is based on that developed by Claypoole, et al.(18). However, it has been found that, in general, adaptive lifting by itself is too flexible to allow the effective distinction of healthy-state and damaged-state vibration signals. Hence, it has been determined that constraints on certain basis characteristics are necessary to enhance the detection of local wave-form changes caused by certain types of gear damage. This processing technique is termed Constrained Adaptive Lifting (CAL).

4.2. The Lifting Scheme

The lifting scheme was developed by Sweldens in the early 1990s as a method for creating new biorthogonal wavelets in settings where the Fourier transform could not be used(16), such as on bounded domains and on curves and surfaces. In later work, Sweldens and Daubechies demonstrated that all perfect reconstruction filterbanks could be formed with a sequence lifting steps(37).

An understanding of the lifting scheme can be best attained by considering the mechanics of lifting from the perspective of the wavelet transform. The fundamental idea behind the wavelet transform is to create a sparse approximation of a given signal using a set of basis functions that exploit the correlation present in the signal. The result of the transform is an approximation of the signal and a measure of the difference between the approximation and the original signal, referred to as the detail. The classical wavelet transform takes advantage of the Fourier transform to construct this approximation in the frequency domain. Lifting achieves the same result while operating exclusively in the time domain. A lifting step consists of three stages: split, predict, and update. Consider a signal $\mathbf{X} = (X_k)_{k \in \mathbf{Z}}$ with $X_k \in \mathbf{R}$.

Split: The splitting stage separates the signal into two disjoint sets $\mathbf{X}_e = (X_{2k})_{k \in \mathbf{Z}}$ and $\mathbf{X}_o = (X_{2k+1})_{k \in \mathbf{Z}}$, consisting of the even and odd indexed samples, respectively. These sets are referred to as polyphase components of signal \mathbf{X} .

Predict: The prediction stage attempts to use \mathbf{X}_o to predict \mathbf{X}_e as

$$\mathbf{X}_e = P(\mathbf{X}_o), \quad (24)$$

where P is the prediction operator (predictor). If the prediction could be performed exactly, then \mathbf{X}_e could be eliminated since it could be easily recreated using P . However, in reality we need to define a measure of the difference between the predicted and actual \mathbf{X}_e . This measure is called the detail \mathbf{d} and is given by

$$\mathbf{d} = \mathbf{X}_e - P(\mathbf{X}_o). \quad (25)$$

In general, the predictor is designed to suppress the low order polynomial signal structure within the detail, preserving the high order structure. This is equivalent to preserving the high frequency signal structure. For example, let the prediction operator be first order (linear) polynomial interpolation. This is referred to as an $N = 2$ point prediction since two points from X_o are used to predict the point of X_e under consideration. The predictor is then given as

$$P(\mathbf{X}_o) = \frac{1}{2}(X_{j,2k-1} + X_{j,2k+1}) \quad (26)$$

The resulting detail is given as

$$d_{j-1,k} = X_{j,2k} - \frac{1}{2}(X_{j,2k-1} + X_{j,2k+1}) \quad (27)$$

Thus, in this case, the detail is the extent to which the signal fails to be linear.

Update: Finally, in order to maintain acceptable frequency characteristics in \mathbf{X}_o , it is necessary to reduce the effect of aliasing introduced by the initial data split. To accomplish this, we introduce the update operator U

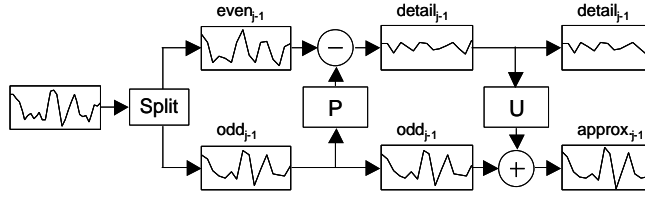


Figure 30. The lifting scheme block diagram.

that uses \mathbf{d} to preserve some frequency properties of \mathbf{X} in \mathbf{X}_o . In practice, U serves to smooth \mathbf{X}_o . The resulting signal, referred to as the approximation \mathbf{a} is given by

$$\mathbf{a} = \mathbf{X}_o + U(\mathbf{d}). \quad (28)$$

This update operation serves to suppress the high order polynomial signal structure within the approximation, while preserving the low order structure, equivalent to preserving the low frequency signal structure. Returning to the example, the update operator is given as

$$U(\mathbf{d}) = \frac{1}{4} (d_{j-1,k-1} + d_{j-1,k}) \quad (29)$$

This is an $\tilde{N} = 2$ point update. The approximation is thus given as

$$a_{j-1,k} = X_{j,2k+1} + \frac{1}{4} (d_{j-1,k-1} + d_{j-1,k}) \quad (30)$$

In this case, the update operator preserves the average of the original signal in the approximation. The lifting scheme block diagram is given in figure 30.

If the prediction and update operators are restricted to be translates and dilates of a single function, then the approximation and detail resulting from one lifting step are equivalent to the approximation and detail produced by one iteration of the wavelet transform. However, no such restrictions must be imposed on lifting, and thus wavelets can be constructed in settings where the Fourier transform cannot be used, such as on bounded intervals.

In the above discussion of the lifting scheme, the role of the basis functions i.e. the wavelet and scaling functions, is not immediately obvious. However, given that \mathbf{d} and \mathbf{a} are equivalent for both the wavelet transform and the lifting scheme, it can be seen that the individual d_k and a_k are the wavelet and scaling function coefficients, respectively. For instance, the linear predict/average preserve implementation of the lifting scheme used in the example is equivalent to the biorthogonal (2,2) wavelet transform of Cohen-Daubechies-Feauveau.

4.3. Adaptive Lifting

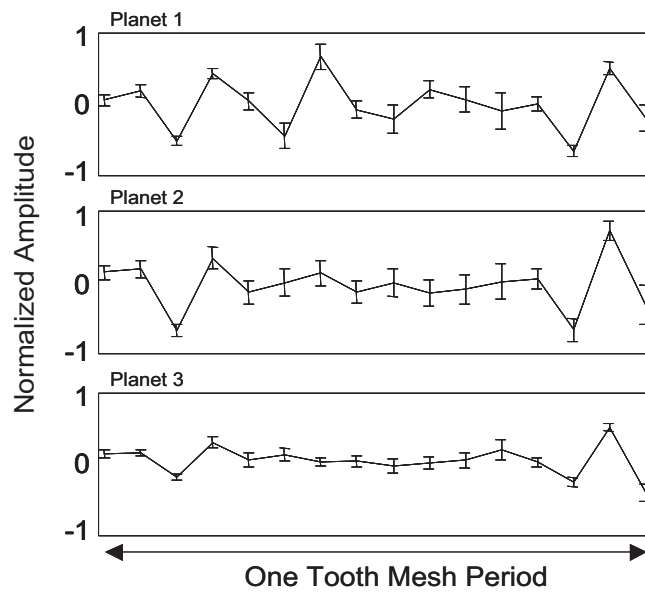
It has been proposed that a wavelet system that shapes itself to the signal under consideration could be more robust and useful in classification problems. This adaptation property enables the creation of a general diagnostic

algorithm that is able to select a set of wavelet basis functions from multiple dictionaries and then use the chosen bases as a phenomenological model of the vibration signals obtained from a specific transmission under a given operating condition. Since the model exists within the framework of a specific analysis technique (i.e. the wavelet transform), the model can be easily compared with vibration signals obtained from the transmission under operation by analyzing the signal using the selected bases.

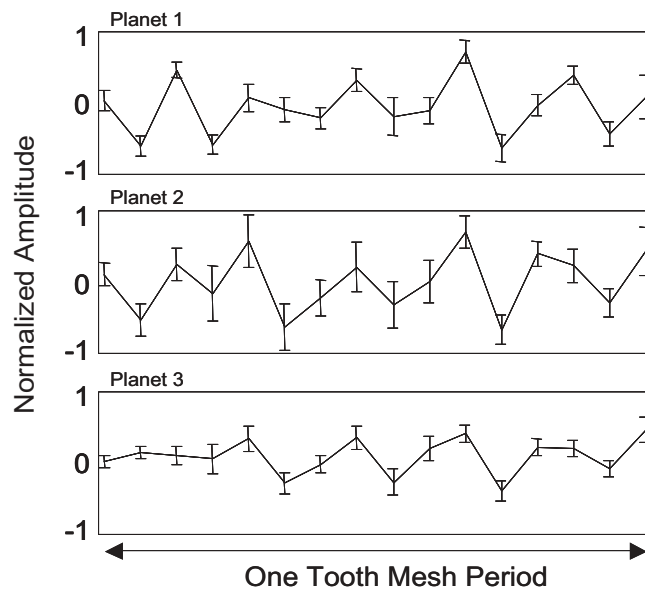
More specifically, if a dictionary can be constructed for a vibration signal obtained from a given transmission in an undamaged condition, then the damage detection algorithm should be less sensitive to any vibration characteristics unique to that transmission. Accordingly, the algorithm should be more sensitive to changes in the vibration signal associated with damage. Adaptive lifting provides a method by which dictionaries tailored to a specific data set can be created.

The key to adding adaptivity to the lifting scheme lies in the method by which the prediction operator P is chosen. In classical lifting, the chosen predictor remains constant (this is equivalent to using a single wavelet dictionary). However, to incorporate adaptivity, it is necessary to allow the predictor to vary such that the resulting representation is locally optimal in some sense. Claypoole, et al. (18), present a method for adapting the predictor referred to as the Space-Adaptive Transform (SpAT). Recall that in the above example, the prediction operator is linear interpolation. The fundamental idea behind SpAT is that higher order interpolating polynomials are also considered at each point in the signal, and the polynomial that provides the best prediction (minimum prediction error) at a given point is chosen as the prediction operator at that point. SpAT uses an $\tilde{N} = 1$ update in conjunction with an $N \in \{1, 3, 5, 7\}$ point prediction. However, for transmission diagnostics, the detail is the primary result of interest, so the update is disregarded beyond this point.

A diagnostic technique based on the adaptive lifting work of Claypoole(18) has been developed by Samuel and Pines(14). In some cases, it was observed that the model, developed using healthy-state transmission vibration data, was able to effectively represent other sets of healthy-state data while failing to effectively represent the damaged-state vibration signal. The result was a small prediction error in the healthy-state case and a large prediction error in the damaged-state case (see figure 31). Thus it was shown that the prediction error could be potentially used to indicate the presence of damage. However, it has subsequently been found that, in many cases, adaptive lifting by itself yields a model that is too flexible to allow the effective distinction of healthy-state and damaged-state vibration signals. Hence, it has been determined that constraints on certain basis characteristics are necessary to enhance the detection of local wave-form changes caused by certain types of gear damage.



(a) Healthy-State.



(b) Damaged-State.

Figure 31. Prediction error for each planet.

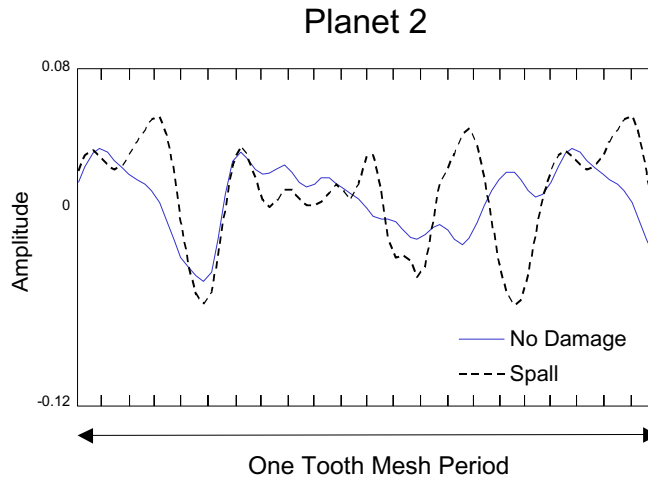


Figure 32. Effect of damage on wave-form.

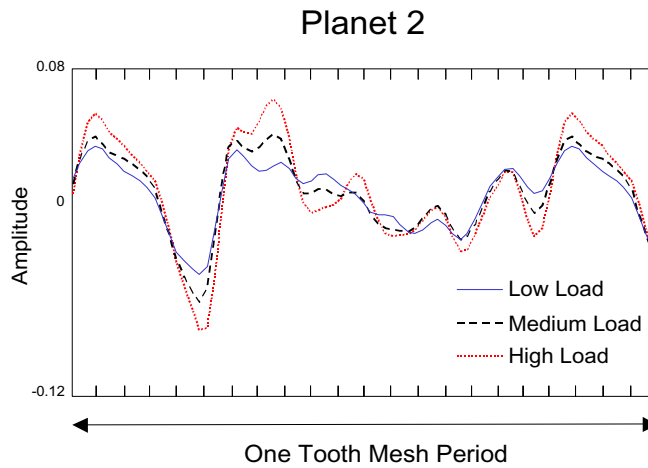


Figure 33. Effect of load variation on wave-form.

4.4. Constrained Adaptive Lifting

The fundamental idea behind the CAL algorithm is the reduction of the order of the functions that form the predictor. It has been observed that certain types of gear damage, specifically tooth face damage, can yield higher order changes in the vibration signal wave-form. By reducing the basis function order, the model becomes inflexible to higher order changes in the shape of subsequent signals under analysis. Figure 32 shows the effect of tooth face spalling on the wave-form of an individual tooth mesh. However, the constraints should still allow the model to be flexible to amplitude changes in the wave-form resulting from load variations. Figure 33 shows the effect of load variations on the wave-form of an individual tooth mesh.

The methodology analyzes individual tooth-mesh wave-forms from a healthy-state gearbox vibration signal that was processed a priori using the vibration separation algorithm. Once again, the polyphase transform is

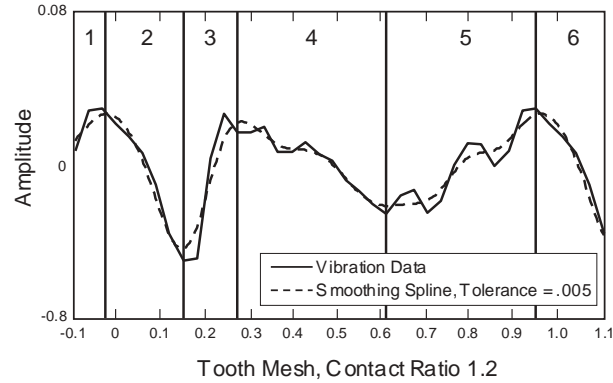


Figure 34. Individual tooth mesh waveform with representative analysis domain indicated.

applied to each waveform. The zeros of the first derivative (slope) and second derivative (curvature) of \mathbf{X}_o are approximated using a smoothing spline. The tolerance for the smoothing spline is chosen to provide a reasonable number of domains. However, a coupling has been noticed between the choice of tolerance and the sensitivity of the algorithm to damage. This coupling merits further study and suggests the use of a time-varying tolerance not implemented in this report. The slope inflection points are used to designate the analysis domains over which the slope remains approximately constant, and the curvature inflection points within each domain are recorded for subsequent use. Figure 34 shows a typical waveform associated with a single tooth mesh of a planet gear. A representative analysis domain is indicated.

An approximate method for selecting the bases is called for due to the approximate nature of the domain selection. Hence, in each analysis domain, the basis is chosen as the lowest order least squares spline approximation of the odd data points that effectively minimizes the prediction error in the l_2 sense. The curvature inflection points within each domain are used as break points for the spline. A coupling has been observed between the maximum model order considered and the sensitivity of the algorithm to damage. Higher order splines tend to be more effective in regions where the analysis domain has not been sufficiently constrained, i.e. the smoothing spline tolerance is not sufficiently tight to capture the higher order nature of the signal. Thus there is a combined coupling between the tolerance, the model order, and the damage sensitivity. This coupling requires further investigation.

The resulting set of bases is used to analyze future-state vibration signals and the prediction error is inspected. It is anticipated that the constraints will allow the transform to effectively adapt to global amplitude changes, yielding small prediction errors. However, local wave-form changes associated with certain types of gear damage should be poorly adapted, causing a significant increase in the prediction error.

4.5. Diagnostic Algorithm

In conjunction with vibration separation, CAL can be used as part of a technique for detecting damage in a helicopter transmission. The framework for this diagnostic methodology is as follows.

Collect and separate: As stated previously, any vibration data collected from a helicopter transmission is a composite of vibrations associated with all of the components within the transmission. Hence, before any diagnostics is performed, the vibrations associated with specific components of the transmission must be isolated and extracted. The vibration separation algorithm is an effective method for attaining this goal.

Adapt: In order to improve the performance of a diagnostic algorithm, some method should be found to tailor the algorithm to a given transmission. In the case of wavelet-based diagnostic algorithms, a set of wavelets that capture the unique vibration characteristics of the transmission is desired. The CAL diagnostic algorithm can perform this function. Vibration data is initially collected from a healthy-state transmission. This data is subsequently used, in conjunction with CAL to develop a predictor that acts as a model of the transmission vibration signal waveforms.

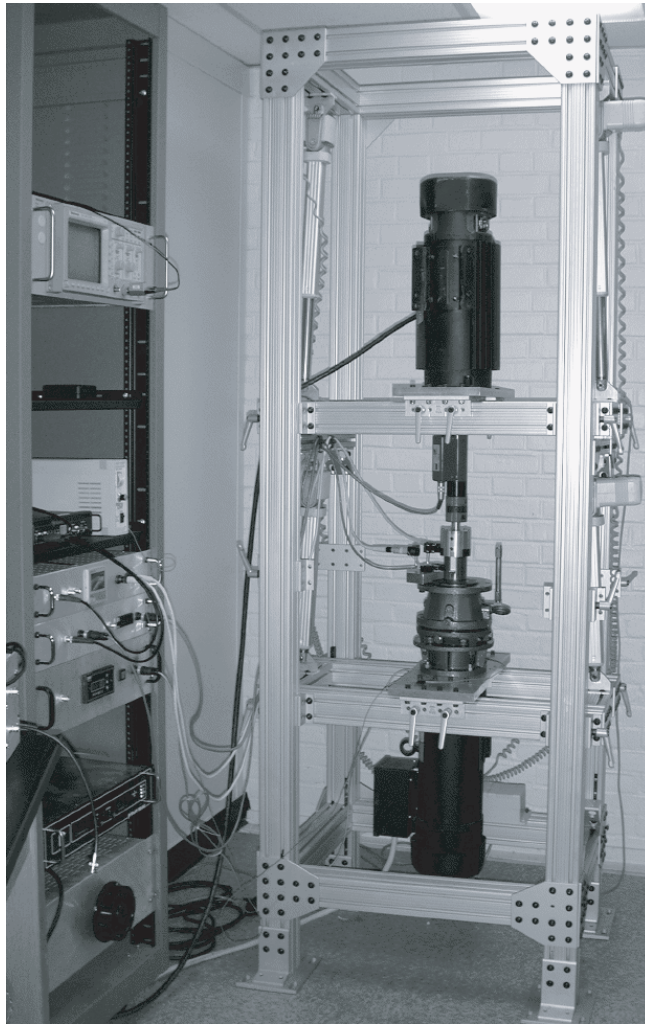
Compute prediction error: During operation of the transmission, CAL is used to process the separated vibration data using the predetermined predictor and analysis domains. The amplitude of the prediction error provides an indication of the presence or absence of certain types of gear damage.

Ultimately, the expected result of this methodology is a physically meaningful vector that changes significantly in the presence of damage.

4.6. Experimental Results

The vibration data used for this work was collected from the University of Maryland Transmission Test Rig (UMTTR) (see figure 35). The gear box used in the UMTTR is an Emerson Gearing PlanetPower single stage planetary reduction gear box with a reduction ratio of 3.84:1. The ring gear has 71 teeth, the sun gear has 25 teeth, and each planet gear has 22 teeth. A hunting tooth ratio exists between both the planet and ring gears and the planet and sun gears. The planet gears are supported by roller bearings. Vibrations are measured using PCB accelerometers mounted around the outside of the ring gear. They are then processed using the vibration separation algorithm with a Tukey window as described in Section 2.

Vibration data was collected from the gear box for both healthy- and damaged-states. Healthy-state data was collected for various load conditions. Data was collected from three damaged-states: planet 2 with one tooth spalled, planet 2 with 5 consecutive teeth spalled, and planet 2 with all teeth spalled. In each case, planet 2 was placed in the gearbox and the position and rotation index monitored in order to keep track of the location of



(a) Test Stand.



(b) Inside Gear Box.

Figure 35. University of Maryland Transmission Test Rig (UMTTR).

the damaged teeth. In the first case, the damaged tooth was positioned such that the damage would appear on tooth 18. In the second case, the damage would appear on teeth 16 through 20.

The vibration separation algorithm was applied to each data set yielding a vibration signal for each planet. CAL was then applied to one set of healthy-state vibration signals under the low load condition and a predictor was found for each planet. Healthy-state vibration signals from the low, medium and high load conditions as well as the damaged-state vibration signals were then analyzed using CAL in conjunction with the previously chosen predictor.

Figures 36, 37, and 38 show the effect of varying load on the CAL prediction error. A small coupling is observed between load level and prediction error amplitude. This coupling is small and would not have a significant effect on the detection of the damage cases considered in this paper. However, it could potentially decrease the sensitivity of the methodology to less severe damage. Hence, further work is necessary to reduce or eliminate this coupling.

Figures 39, 40, 41 and 42 show the vibration signal and CAL prediction error for each damage case. It should be noted that there is some variation in the effectiveness of the modelling between each planet. In particular, the damage on planet 2 tends to slightly corrupt the planet 3 vibration signal. This phenomenon requires further study. However, in each case, the damage is clearly evident on planet 2 in the expected location.

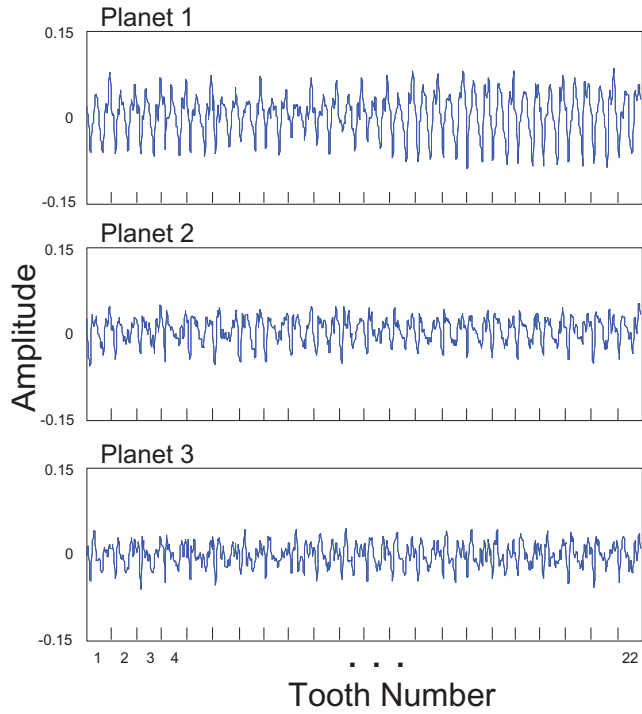
These results show that CAL is potentially beneficial for transmission diagnostics. However, further investigation is required to better validate the performance of the algorithm. In addition, a method to better quantify the output of the algorithm should be developed.

5. CONCLUSION

This report describes a set of methodologies for damage detection in a planetary transmission. A technique for extracting the vibration signals associated with the sun and planet gears of a planetary transmission developed by McFadden was presented and issues associated with the implementation of the methodology were discussed. An generalization of the technique was developed for use with vibration signals collected from multiple transducers located around the ring gear. Selection of an appropriate window function for use with the vibration separation technique was discussed, and it was determined that a moderately narrow Tukey window had the most desirable properties.

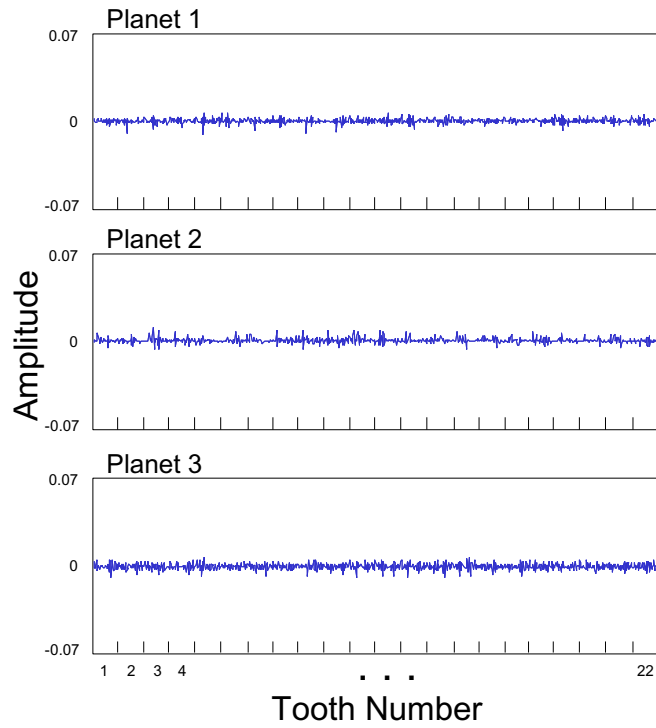
Following the theoretical development of the vibration separation technique, real-time implementation was discussed, and a real-time code using LabVIEWTM was developed. The code and associated manual are included with the report.

Separated Data



(a) Separated Vibration Signals.

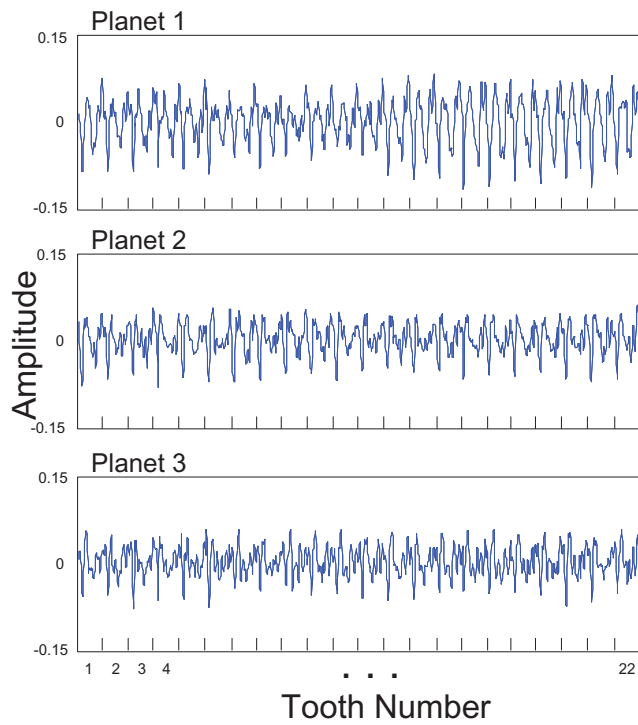
CAL Output



(b) CAL Prediction Error.

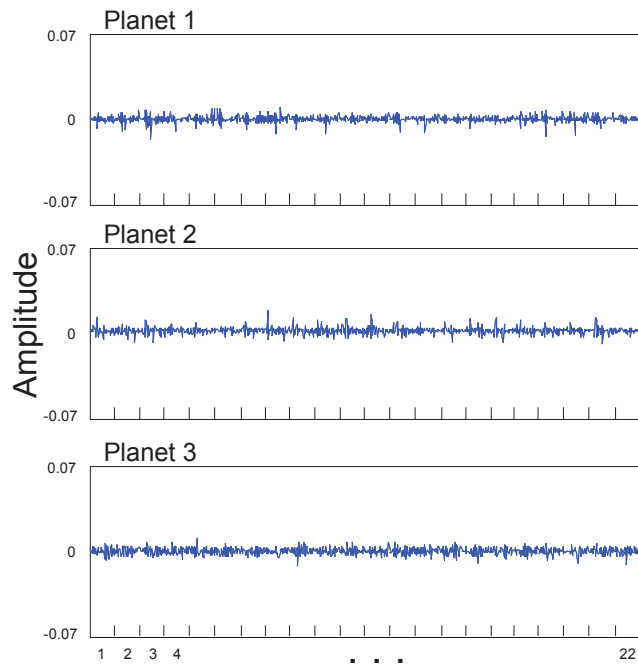
Figure 36. Healthy State, Low Load.

Separated Data



(a) Separated Vibration Signals.

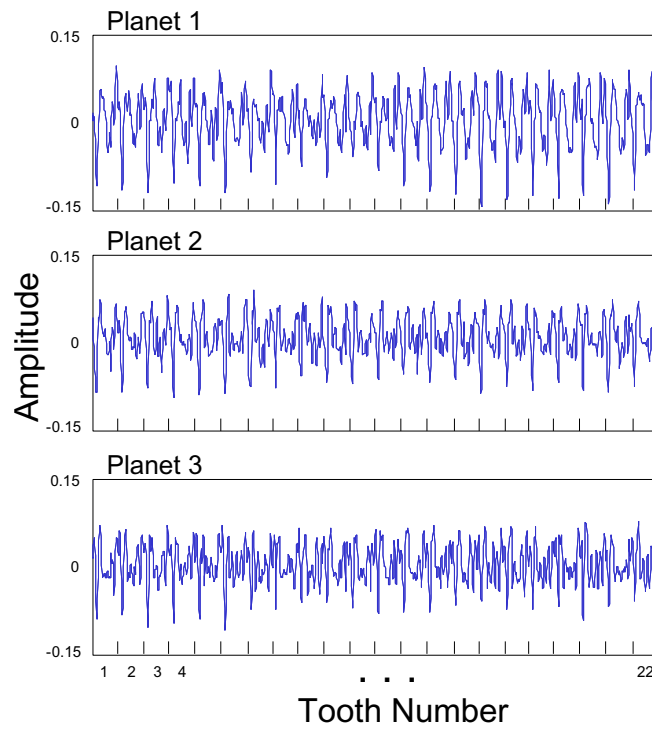
CAL Output



(b) CAL Prediction Error.

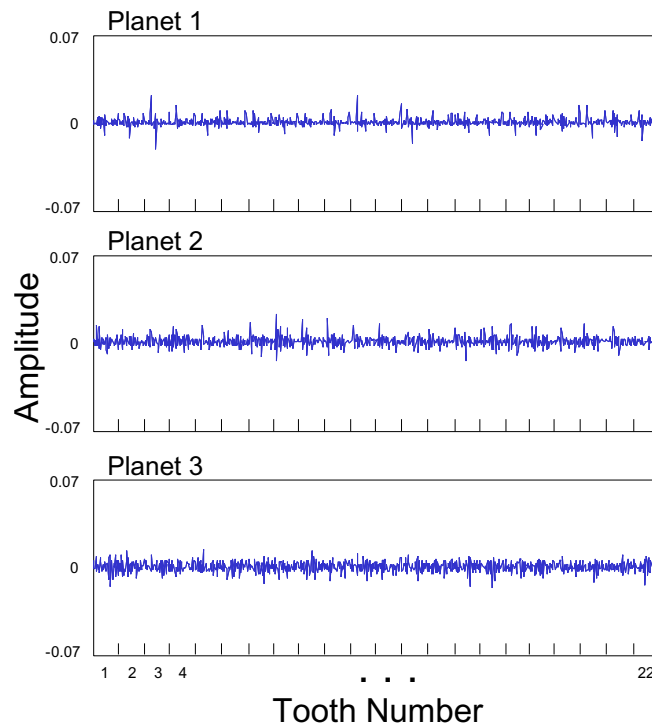
Figure 37. Healty State, Medium Load.

Separated Data



(a) Separated Vibration Signals.

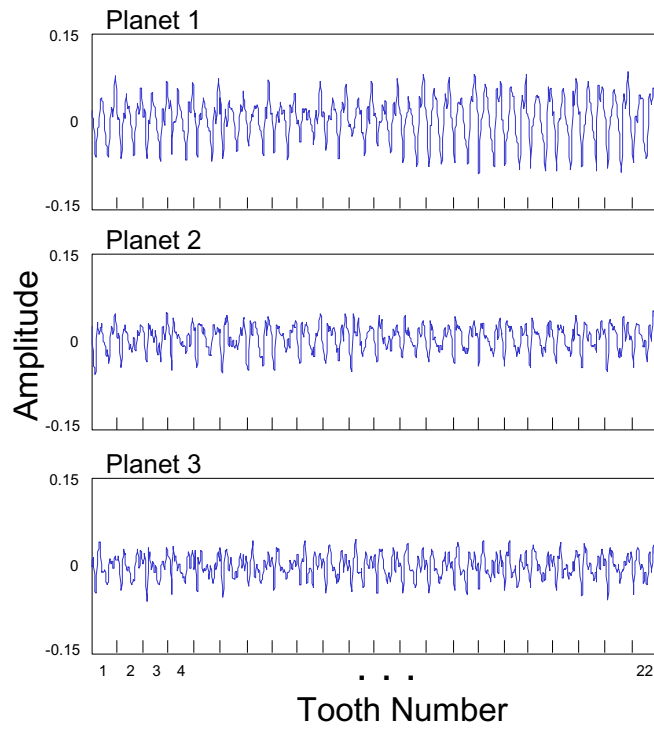
CAL Output



(b) CAL Prediction Error.

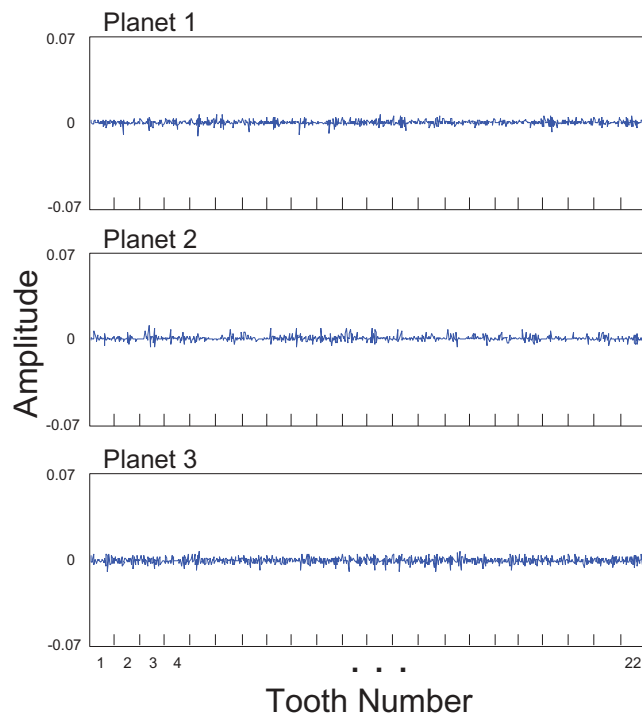
Figure 38. Healty State, High Load.

Separated Data



(a) Separated Vibration Signals.

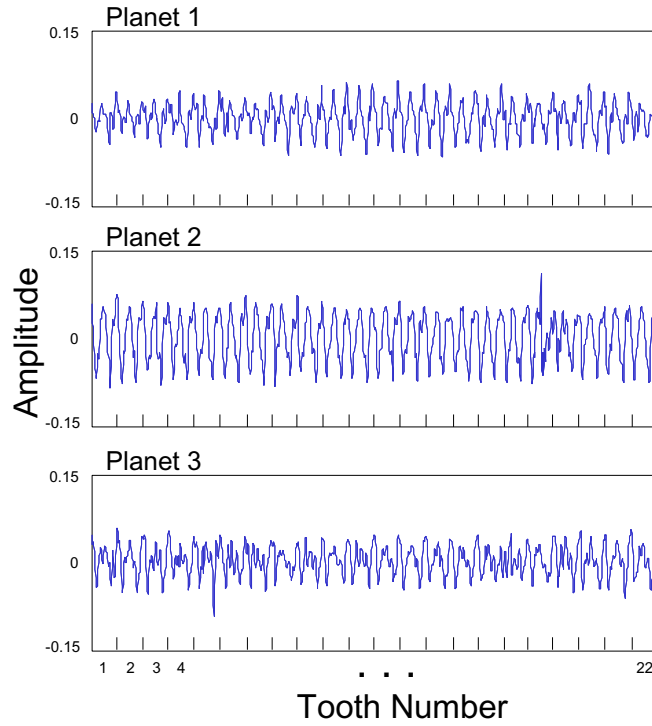
CAL Output



(b) CAL Prediction Error.

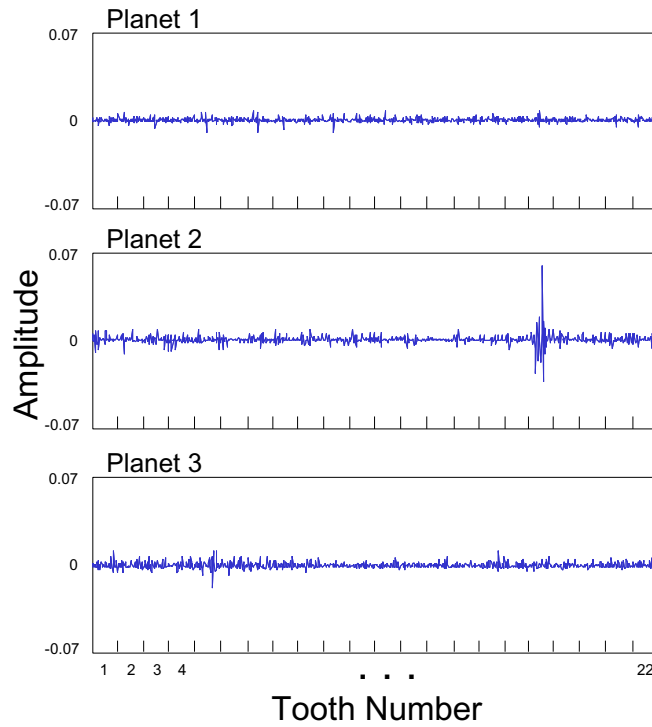
Figure 39. Healthy State.

Separated Data



(a) Separated Vibration Signals.

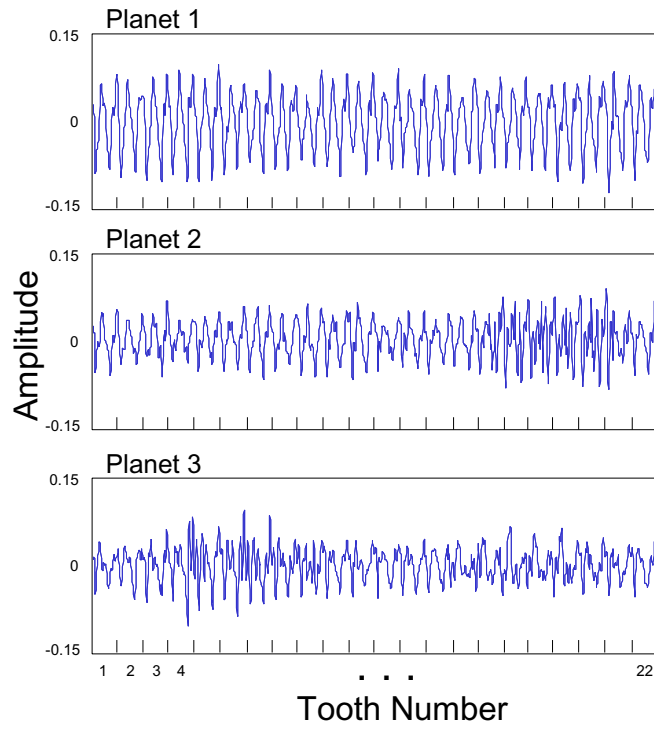
CAL Output



(b) CAL Prediction Error.

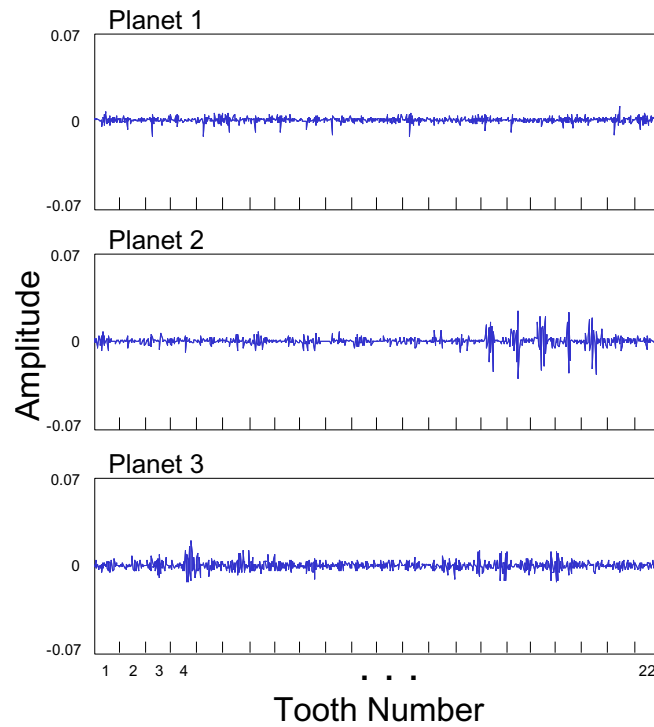
Figure 40. One Tooth Spalled on Planet 2.

Separated Data



(a) Separated Vibration Signals.

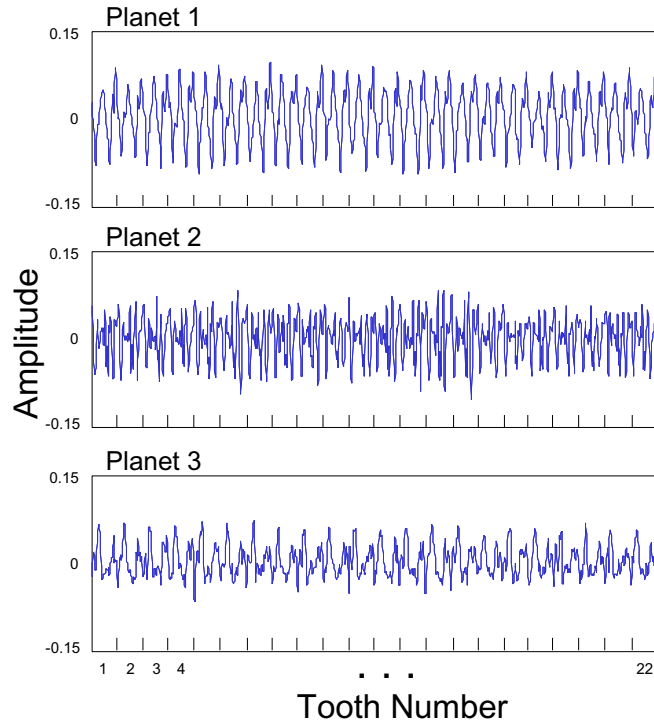
CAL Output



(b) CAL Prediction Error.

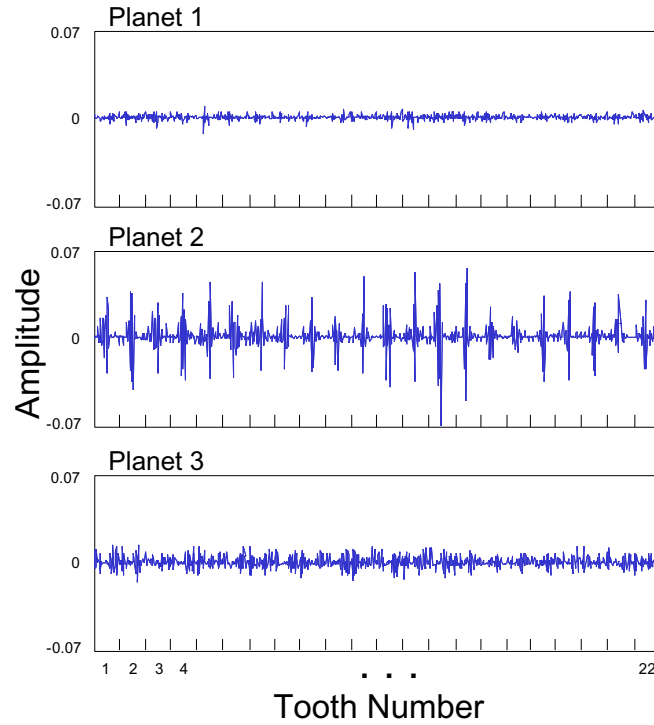
Figure 41. Five Teeth Spalled on Planet 2.

Separated Data



(a) Separated Vibration Signals.

CAL Output



(b) CAL Prediction Error.

Figure 42. All Teeth Spalled on Planet 2.

Finally, a new diagnostic technique based on constrained adaptive lifting (CAL) was presented and an initial validation study was performed using data collected from the University of Maryland Transmission Test Rig. In time, the CAL diagnostic algorithm will be incorporated into the real-time LabVIEW[™]-based code.

APPENDIX A

MANUAL FOR LabVIEW™-BASED VIBRATION SEPARATION CODE

A.1. Setup

A.1.1. Software

The latest enhancements to this diagnostic program, effectively creating version 2.3, include various interface changes and additional metrics, without changing much of the program's core, which has been experimentally validated. Listed below are the various capabilities of the latest iteration of the program.

- **Ability to customize NA4* acquisition:**

A user can specify the variance, (denominator for NA4*), used for diagnostic computation. Four settings are available: *Collect*, *Recall*, *None*, and *Locked Denominator*. *Collect* mode begins time averaging the variance and computes the NA4* value based on the current averaged value for the variance. The final averaged data from *Collect* mode is saved to a spreadsheet file. The data saved using *Collect* mode can be read during a subsequent acquisition using *Recall* mode. While in *Collect Mode*, vibration data would be acquired from a system containing entirely healthy components. Then, one or more healthy gears would be replaced with gears containing known seeded faults, where the NA4* variance values from the healthy data, known a priori, would remain constant during the next test. NA4* values would then react more effectively to damage. This procedure was developed originally to accommodate testing rigs lacking sufficient torque to damage gears progressively, but will presumably be insightful for investigating the vibration changes due to particular types of faults which must be seeded beforehand. Should the NA4* input be set to *None*, the acquisition will proceed as it would in *Collect* mode, but will not save a *variancematrix.txt* file.

- **Output Format:** At the time the program is run, the user will be asked to specify a new folder, designated the *Test Run Folder*, into which all the collected data from the test will be stored. In order to keep unnecessarily complicated options to a minimum, the user is not given the option of saving or not saving most files, with the exception of saving raw data, which creates considerably large files. After a test, the *Test Run Folder* contains a new folder called *Metrics*. Within this folder there is one spreadsheet .txt file for each metric calculated for both the planet and sun gears. If the NA4* selection was set to *Collect*, then a file called '*variancematrix.txt*' is created to contain the saved variance values. Each assembled and averaged planet vector is contained in the *Planet Vectors* folder, with the order in which each was collected being denoted by its numerical suffix. A similar folder called *Sun Vectors* contains the sun vectors. Should the user wish to save the Raw Data, a folder designated *RawData* is created which contains spreadsheet .txt files. Each Raw Data file contains a numeric suffix. Each Raw Data file contains the necessary Raw Data to re-create a single averaged, assembled planet vector. Each numerical suffix on a RawData file

indicates that RawData file created the planet vector of the same suffix in the *Planet Vectors* folder. Finally, two files regarding the program's set parameters are saved. One is designated *parameters.txt* and another *savedsettings.txt*. The user may refer to the *savedsettings.txt* file information regarding the test, including any pre-test notes input on the front panel. The *parameters.txt* file is saved so that in the future, a user, instead of re-entering most of the parameters on the front panel, can select one of these files and the parameters set from a past acquisition can be reused. This feature is only very useful when taking data from a variety of systems often.

- **Input Format:**

In addition to the obvious capability of acquiring signals from the DAQ card in real-time, the program can also read saved raw data spreadsheet files from previous acquisitions, essentially re-creating earlier acquisitions. The useful aspect, though is the ability to change certain parameters, such as window type or width, and rerunning the data to examine changes. The only restriction is that the scan rate will always be the scan rate from the original acquisition. The other useful aspect of this feature, is that any data from any source can be read into the program and processed. The input must be a spreadsheet file **named 'RawData0.txt'**, TAB delimited, with 2 to 5 columns, where the first column is the 1/rev pulse train, and the other columns are the sensors. To acquire more than one averaged planet vector from the raw data, set the Repeater Switch to the number of desired planet vectors and set the acquisition switch to average a number of times equal to the number of sun teeth. Note that this will only work if a hunting tooth ratio exists between the planet gears and ring gear. If data needs to be formatted to fit the spreadsheet specification, MATLAB can be used to manipulate the data into columns and then the command, 'save data.txt -ascii -tabs' used to create the input file.

This version of the Planetary Gear Diagnostic Program was written using LabVIEW 6.1. Earlier versions of LabVIEW will most likely have trouble opening the program. Currently, the program supports up to 4 planets and 4 sensors. The Graphical User Interface is best viewed at a screen resolution set to 1600 X 1200. The program is started by running the .VI file names *MAIN.vi*. All other VI's are internal to the structure of *MAIN.vi*.

A.1.2. Hardware

This program was developed and tested using a 6062E PCMCIA card from National Instruments. Any other NI board should, but of course cannot be guaranteed to, work perfectly without any modifications to the program. The program was designed to function minimally using only analog input channels. The *Acquisition Sync Hardware Trigger*, meant to ensure continuity between runs, has been made optional in order to minimize



Figure 43. Diagnostic System

hardware conflicts, but is suggested in order to gather the most accurate data possible. Figure 43 shows an overview of the order for system setup.

A.2. Main Front Panel

When *MAIN.vi* is opened, the primary front panel displays all the available input options and output readings. The following program inputs and outputs are organized according to their functions.

- Stop:** Stop the acquisition. The *Stop* button can be hit at any time during an acquisition. If the optional acquisition switch (see subsection “Blue: Optional Inputs”) is set to acquire a certain number of averages, the program will stop itself upon the completion of the requisite number of averages. Note: when the hardware trigger option (see subsection “Blue: Optional Inputs”) is switched on and the program is running, the hardware pulse must start the acquisition before the *Stop* button can be used. Otherwise, the full length of time set in *time limit* (see subsection “Blue: Optional Inputs”) must be reached before the program will end and can be started again. This is because the *Stop* button is simply a boolean value wired to the program’s while loops. If the hardware trigger never starts the acquisition and hence the loops, the loops cannot iterate and hence the program cannot be stopped by software means.

A.2.1. Pink: Required Input

The required input section of the program is shown in figure 44.

- Device No.:**

The default setting for *device no.* is 1. Should the DAQ card be configured on the computer as a different device number, this setting must be changed to match. Most systems will have this value set to 1 unless there are multiple DAQ cards on each machine. If necessary, the device number can be found by pointing to the top of the LabVIEW menu row and following Tools–Data Acquisition–Channel Viewer and clicking on the “Devices” tab.

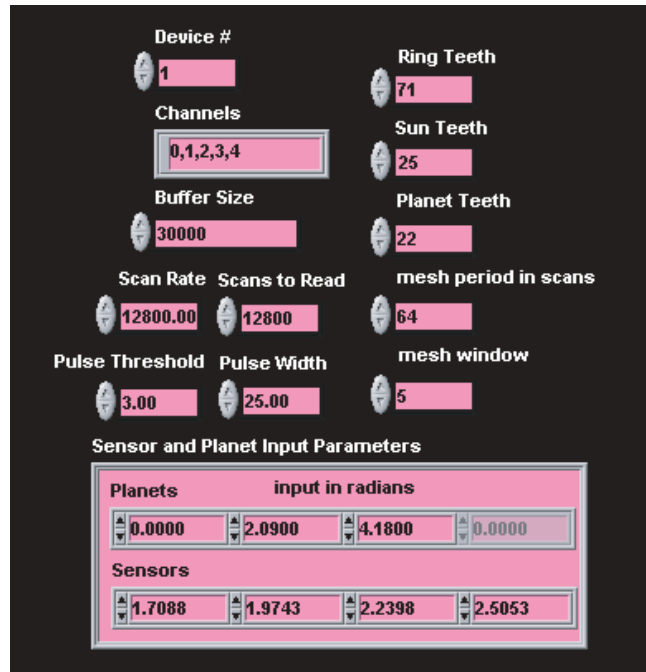


Figure 44. Required Input

- **Channels:**

The *Channels* input defines which channels on the DAQ card are to be used for acquisition. The first channel in the sequence must be the 1/rev pulse train, while the 4 subsequent channels are the sensor input channels.

- **Buffer Size:**

The *Buffer Size* is the amount of designated memory assigned to the hardware buffer. It must be at least the size of *Scans to Read* assuming that *Scan Rate* and *Scans to Read* are set to be the same. It is recommended that *Buffer Size* be set to approximately 2 times the size of *Scans to Read*.

- **Scan Rate:**

The *Scan Rate* sets the machine scanning rate (sampling rate). A higher scan rate provides better signal resolution. However, setting *Scan Rate* too high may result in a detrimental performance lag due to the greater amount of processing. In general, leaving this value at 10000-15000 should be sufficient. A rule of thumb that can be used is to start with the number of samples desired for each tooth mesh, and then find the necessary scan rate, taking the RPM of the system and number of gear teeth into account.

- **Scans to Read:**

This should be set to the same number as the *Scan Rate*. It has not been thoroughly tested any other way. Theoretically, setting this value to half the scan rate would result in an update rate of 0.5 seconds. In the same way, setting this value to twice the scan rate would result in an update rate of 2 seconds. Currently, it is believed that a 1 second update rate is a good compromise between fast updates and a high necessary processing rate that would outpace the computer.

- **Pulse Threshold/Pulse Width:** The *Pulse Threshold* and *Pulse Width* specify the inputs to the pulse finding function that locates the wave front of the 1/rev counter pulses in the incoming buffer. The *Pulse Width* should be OK around 3/1000 of the scan rate. The *Pulse Threshold* should be set to about 3/4 of the expected maximum amplitude of the counter pulse.
- **Ring Teeth/Planet Teeth/Sun Teeth:** These inputs are for the number of teeth on the ring gear, the number of teeth on the planet gears, and the number of teeth on the sun gear, respectively.
- **Mesh Window:** The *Mesh Window* defines the width of the window of data extracted from the raw vibration signal. It must be input in terms of the number of teeth. The window is centered on the planet lobe. This input should be an odd integer; otherwise non-integer tooth coverage will result. The minimum width is 1 and the maximum width is the greatest odd integer less than or equal to the number of planet teeth.
- **Mesh Period:** The *Mesh Period* defines the number of scans per tooth mesh period in the output signal. It is recommended that the value be the smallest power of 2 greater than the number of scans per tooth mesh period in the raw data. The scans per tooth mesh period in the raw data can be computed by dividing the *Scan Rate* by the nominal operating rotational frequency of the planet carrier (in rotations per second) and then dividing by the number of teeth on the ring gear.
- **Sensor and Planet Input Parameters:** This set of inputs defines the location of the sensors and planets relative to each other at the point in time when the wave front of the 1/rev pulse is encountered. The first planet is defined as the planet that will first pass sensor 1. Sensor 1 is defined as the first sensor passed by the first planet. The first planet is set to zero radians. Subsequent planets are input as the distance in radians away from the first planet, positive against the direction of the rotation of the gearbox. This allows for asymmetric planet spacing, such as may be encountered on certain gearboxes. The sensors are input as the distance in radians away from the first planet, positive in the direction of rotation of the gearbox. Figure 45 illustrates a gear train with 3 equidistant planets and 3 sensors.

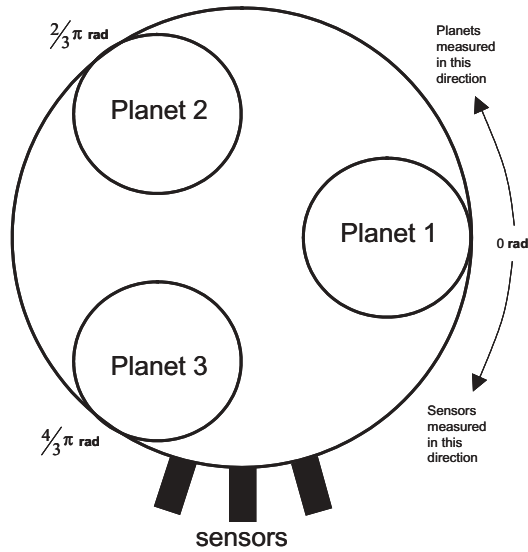


Figure 45. Sensor and Planet Location Designations

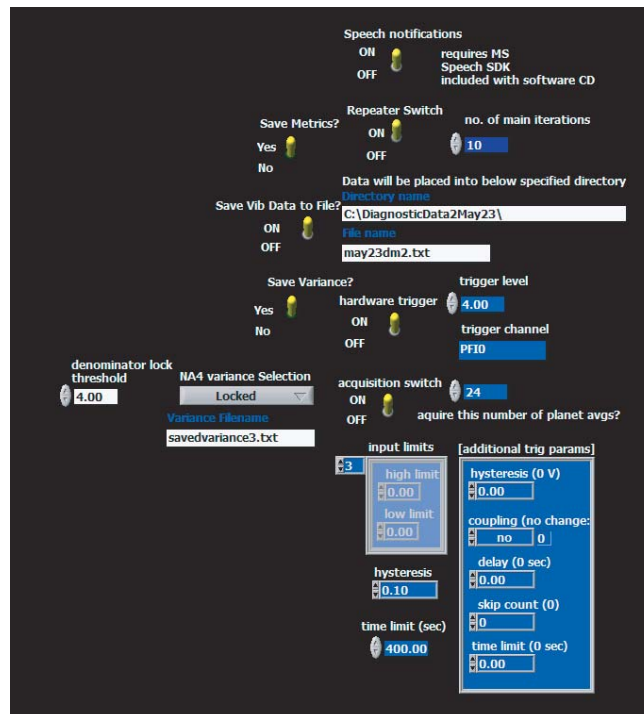


Figure 46. Optional Input

A.2.2. Blue: Optional Input

The optional input section of the program is shown in figure 46.

- **Speech Notifications:** When enabled, a voice will announce the beginning and end of the data acquisition. This is solely for the convenience of the user and has no detrimental effects if disabled. This function requires Microsoft's speech SDK which is included on the program CD.
- **Repeater Switch:** This sets the total number of averaged, assembled planet and sun vectors to acquire, and hence the total number of metric diagnostic points to acquire. This value has the greatest influence on total acquisition time. In general, for a gear system with a hunting tooth ratio between the planets and ring gear, (*Planet Teeth*) rotations are required to assemble a single planet vector. Each assembled planet vector undergoes averaging until (*Planet Teeth x Sun Teeth*) revolutions have been completed. This final time averaged planet vector produces one metric data point, and hence one data point for any other diagnostic. For the UM Transmission Test Rig, using a 3 planet gear system with 22 planet teeth and 25 sun teeth rotating at about 5.25 Hz, each data point requires about one minute and 45 seconds; and 10 data points require about 18-19 minutes. It is projected that when tests using a new system are conducted that test gears to failure, the program will require a new function that stops the program when failure occurs instead of a set number of repetitions.
- **Read Data from File:** If set to 'On', the program will prompt the user to find the folder that contains the Raw Data to read. Read data currently must be named *RawData0.txt* in order for the program to find it. If this is set to 'Off', the program will begin acquiring from the DAQ as usual.
- **Save Raw Data:** Gives the option of saving the Raw Data that is used to assemble each planet vector. If set to 'Yes', the data will be put into the *Test Run Folder*.
- **Acquisition Synch Hardware Trigger:** This switch, when enabled, looks for a pulse on the PFI0/TRIG BNC port before beginning the acquisition. Once the trigger pulse is found, the acquisition begins as usual. If the *Repeater Switch* is enabled for a value greater than one, once the program acquires the first tooth vector, the program resets the hardware trigger and looks for the next hardware pulse to begin a new Planet Tooth Vector acquisition. One consideration is that if the preceding loop ends too close to the hardware trigger, the program will miss that hardware trigger, and wait for the next. This situation would double acquisition time and for that reason, for tests done on the UM Test Rig, the *number of averages* is set to 24 where the hardware trigger pulses every 25. That gained time corresponding to one average is sufficient to allow the program to reset.

- **Trigger Channel/Trigger Level:** This input sets the channel for the hardware acquisition trigger. The default setting is 'PFI0' as it is expected that an analog hardware trigger is input to the PFI0/TRIG port. The trigger level specifies the trigger value the hardware trigger looks for before it pulses.
- **Time Limit:** The *time limit* should be set to a value, in seconds, that is a longer period of time than the period of the hardware pulse train. In addition, it should not be set too much higher since, should the program acquisition be aborted before the hardware pulse fires, the program will wait until this value expires before timing out and ending the program. The only way to stop the program before this time expires is to give it a hardware pulse or close LabVIEW entirely. Setting this to slightly larger than the period of the hardware pulse train is a good rule of thumb.
- **Acquisition Switch:** Depending on the mode of operation, this may be a necessary input for the application. If the user wishes to stop the current accumulation of teeth vector averages with the stop button, this can be disabled. If enabled, regardless of what the Repeater Switch is set to, the program will acquire the number of averages for the teeth vectors as is specified in this field. For a Repeater Switch value greater than one, once the number of tooth vector averages specified in this field is reached the program either repeats immediately if the hardware trigger is off or waits for the next hardware trigger to acquire another averaged set of teeth vectors.
- **Input Limits:** By entering the expected range of voltages for each of the channels, the effect of quantization is minimized. More about this feature can be found in the DAQ manual for the individual system. The program should work fine with the current settings. Even with a 12-bit board, voltages for +/- 10 volts limits, the DAQ board maximum, are divided into increments of about 0.004 volts, which is more than sufficient.
- **Additional Trig Params:** These are generally best left alone for the program to work fine.
- **Hysteresis:** This also can just be left alone for the program to work fine.
- **NA4 Variance Selection:** 4 options can be chosen here. *Recall*, *Collect*, *None*, and *Locked Denominator*. *Collect* mode begins time averaging the variance and computes the NA4* value based on the current averaged value for the variance. The data from *Collect* mode is saved to a spreadsheet file. *Recall* mode requires the previous acquisition of healthy variance data using *Collect* mode in the form of the spreadsheet file. The new kurtosis values, assumed to be from damaged data, are divided by the recalled values of the variance from healthy data. This will help damaged data to stand out. *Locked Denominator* mode will begin acquiring as in *Collect mode*, by averaging the variance over time. After the variance rises above a

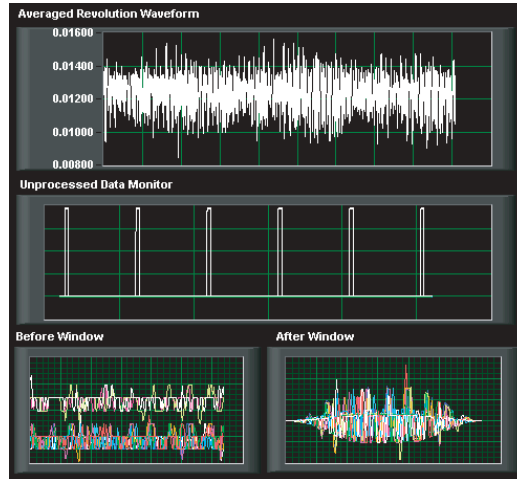


Figure 47. Non-essential Output

certain predetermined value, the denominator “locks” and no further updating occurs. No data is saved to a file in this mode. When *None* is selected, the program operates as in *Collect* mode, but no data is saved to a variance file. When performing a test where a system is run using healthy data and then stopped, opened, and damaged gears are placed inside, the *Collect* and *Recall* modes are ideal. When performing a test beginning with a healthy system and then running it to failure, the *Locked Denominator* case is ideal.

- **Denominator Lock Threshold:** This value specifies the threshold at which the variance in the denominator locks into place. This value is only utilized if the NA4 Variance Selection value is set to *Locked Denominator* mode.

A.2.3. Grey: Non-essential Output

This section, shown in figure 47, provides output that is useful during acquisition, but is not necessary and not sent out to a file.

- **Averaged Waveform:** This output display shows the average of all carrier cycles, (each carrier cycle is delimited by the 1/rev pulses). In the end, it should usually be evident that there are “lobes” equal to the number of planets in the gearbox, due to the increased vibration amplitude that occurs when each planet passes the sensors. This averaged waveform is tapped off the data from sensor 1 only.
- **Raw Data:** This simply shows all of the data, 1/rev pulses and sensors, as it is read from the buffer.
- **Before/After Window:** Shows the segment of data extracted from the raw vibration signal before and after the window is applied. The window can be easily replaced with other windows. Notice that the

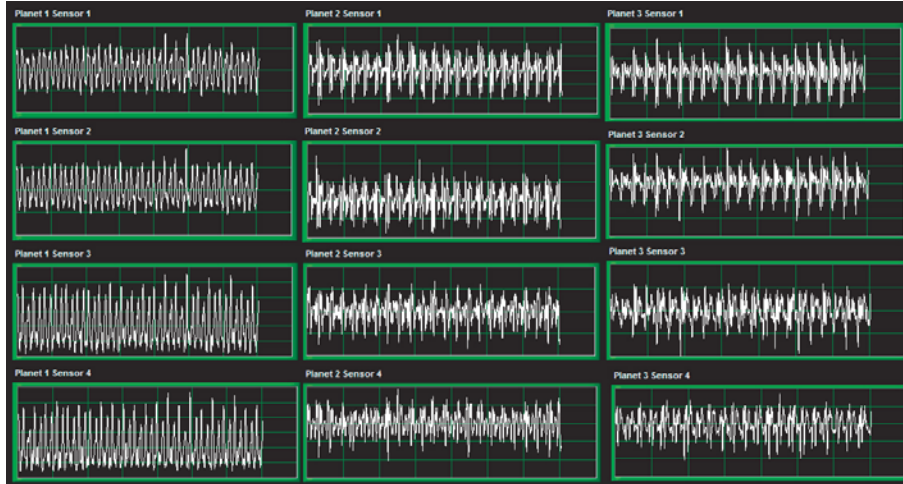


Figure 48. Essential Output

windowing function also centers the mean of the data about zero.

- **Planet Vector Polar Plots:** These plots display the planet vectors associated with sensor 1 plotted over a circle. Currently, this feature only is designed to plot the vibrations associated with each planet over a pictorial representation of a gear. In the future, the hope is to use these plots in a more informative manner.

A.2.4. Green: Planet Output

The essential output section of the program is shown in figure 48.

- **Planet Averages Completed** This keeps count of the number of ensembles that have been averaged to create the final output.
- **Total No. of Waveforms Collected** This displays the total number of revolutions that have been processed since the acquisition began. This value only updates after the entire acquisition has completed.
- **Planet(X) Sensor(Y)** These are the displays for the final output of the program. These windows are what is saved to the spreadsheet file and can be processed. If not all planets or sensors are used these windows remain at zero. When the data is output to the spreadsheet file, the unused windows are all zeros, to act as a placeholder.

A.2.5. Orange: Metric Output

- **Planet/Sun, metric(X)** These graphs display the current outputs from the diagnostic metrics. They are updated every time a diagnostic point is collected.

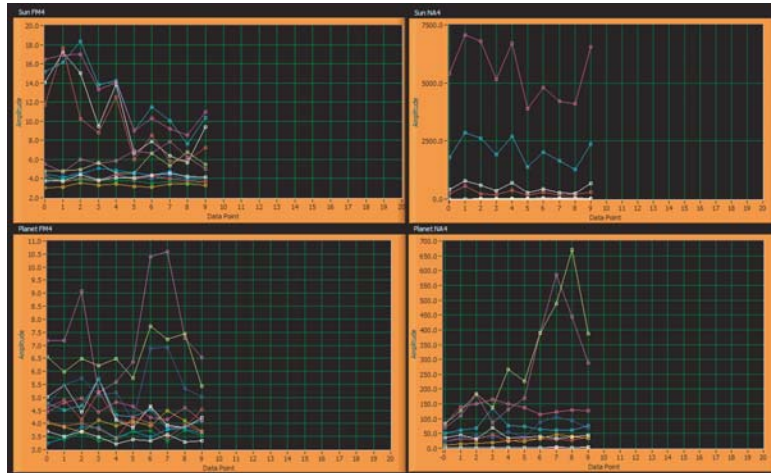


Figure 49. Metric Outputs

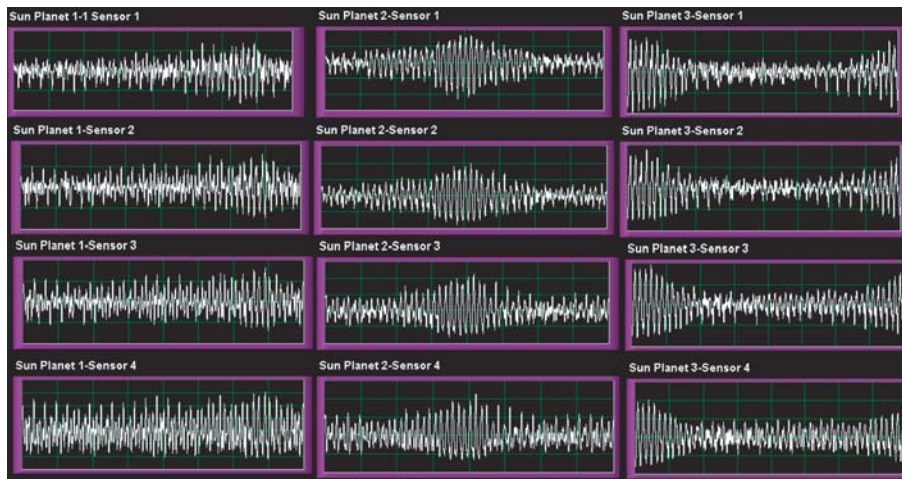


Figure 50. Sun Outputs

A.2.6. Violet: Sun Output

- **Actual Sun Averages** This keeps count of the number of ensembles that have been averaged to create the final output.
- **Calculated Sun Averages** Since the input for the acquisition switch is the number of planet averages, this simply displays the calculated number of sun averages. The calculation is: $(No. of Planet Avgs) \times (Planet Teeth/Sun Teeth)$

A.3. Program Walkthrough

This is the section for the reader who would like to understand the data flow through the program. It is not practical to convert all of the code to jpeg pictures or .eps files to display in a Word or LaTeX document due

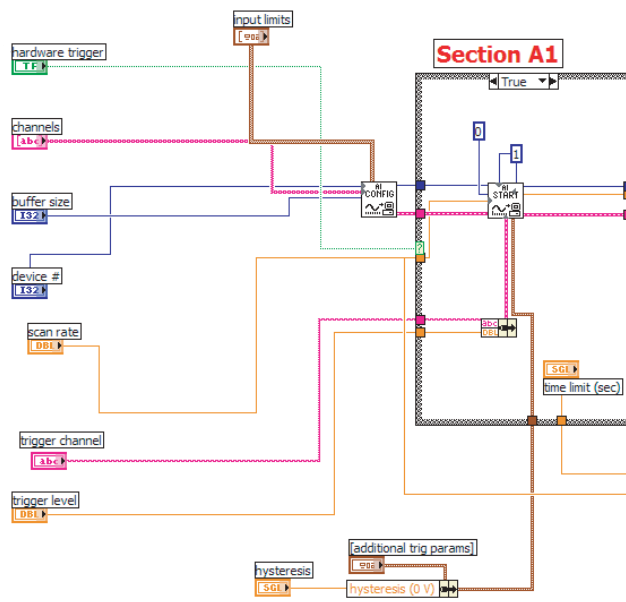


Figure 51. Section A1

to the large size and intricate detail, so it might be helpful to have the code displayed on a monitor during the walkthrough.

- **Section A1:**

Figure 51 shows the first part of the program. The AI Config and AI Start system VIs are the main focus of this section. The options at the left define parameters that are used by both of these VIs. The AI Start VI is in a case statement that switches depending on whether or not hardware trigger is on or off. If on, the AI Start VI waits for a hardware pulse to begin the acquisition. If disabled, the VI begins continuous acquisition immediately when the program is run. Should the *Repeater Switch* be enabled with a value greater than one, this section will be called again for a number of times equal to the value in the *Repeater Switch* field.

- **Section A2:** This loop, shown in figure 52, resides within the main loop. It is responsible for receiving waveforms that represent one revolution of data from one sensor and keeping a continuous weighted average of them. The continuous weighted average is displayed in the averaged waveform window of the grey non-essential output section (see figure 53). Note the three planet lobes that appear in each third of the signal

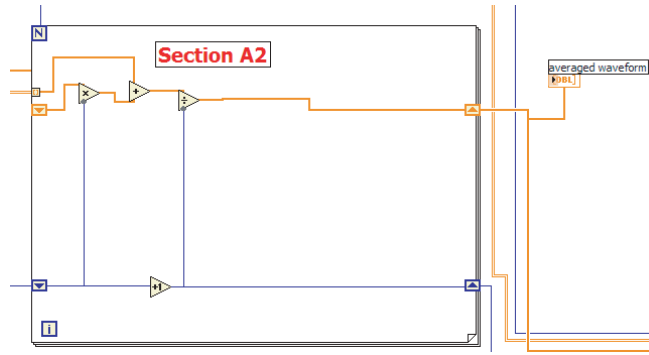


Figure 52. Section A2

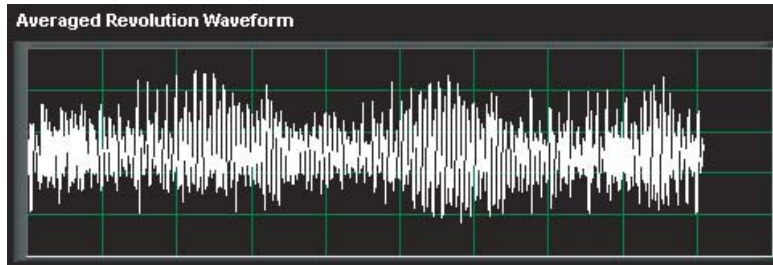


Figure 53. Averaged Waveform Window

in figure 53. In the coming sections, the mesh windows to be extracted will be centered over the positions of these lobes.

- **Sections A3 through A5** The four VIs shown in figure 54 are the main sub VI data processors in this section.

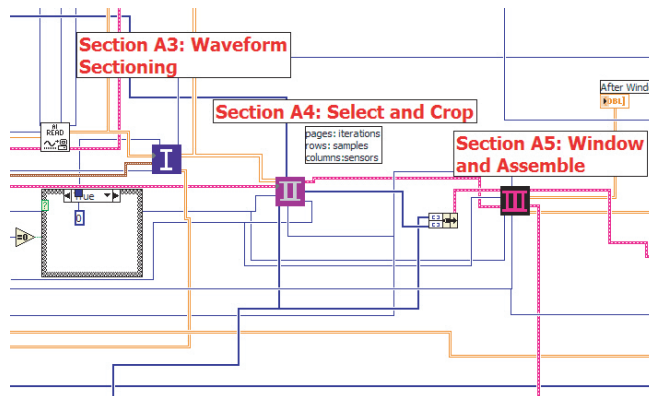


Figure 54. Sections A3 through A5

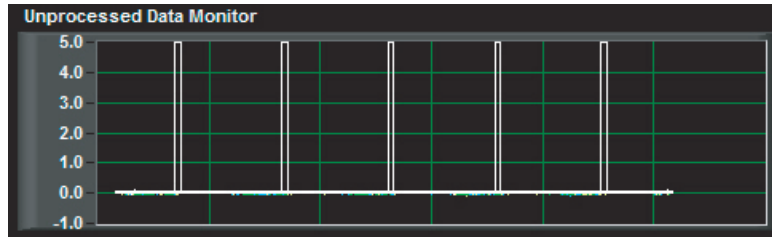


Figure 55. Unprocessed Data Monitor

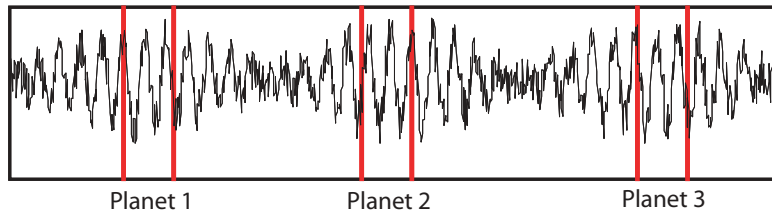


Figure 56. Data Selection

- **AI Read:** Here the data is read from the buffer on a first-in/first-out basis. The data is in the format of 5 columns, the first being the 1/rev pulse, and the next four being the sensors. The data from here is displayed in the unprocessed data monitor (see figure 55).
- **Waveform Sectioning:** Here this raw, unprocessed data is sectioned into individual cycle waveforms, the beginning and end of which are the 1/rev pulses. This VI outputs each revolution of the gear system delimited by the 1/rev pulses. Initially, each waveform is slightly different in length from the others due to slight variations in gear system RPM. An interpolation node is present to adjust all of the waveforms to be the same length. The interpolation constant is mesh period times ring teeth, which gives the entire number of scans per revolution.
- **Selection and Cropping:** In this VI, the locations of the centers of the lobes, determined from sensor and planet input parameters, are used to select segments of data, one for each planet, of size mesh window, centered about each lobe. This yields a segment of data, referred to as a mesh window, for every planet and sensor. The process is visualized through the graphic in figure 56, where a one-tooth width mesh window section for planet three is between the two vertical lines.
- **Windowing and Assembly:** In this VI, a window function is applied to the mesh windows from the previous VI. This serves to minimize discontinuities resulting from the assemble process covered in the next section. The window type is interchangeable and the default window is shown in figure 57.

A typical set of data segments is shown in figure 58.

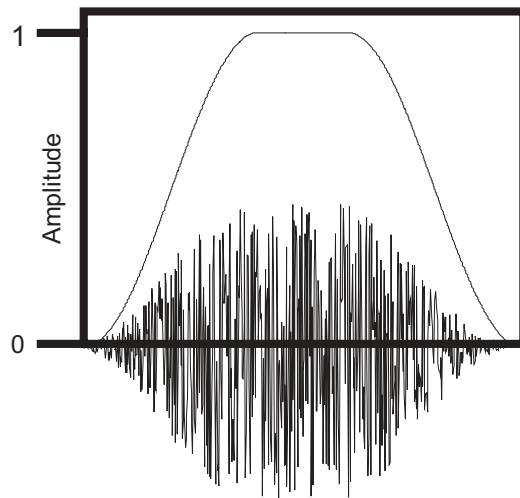


Figure 57. Default Windowing Function

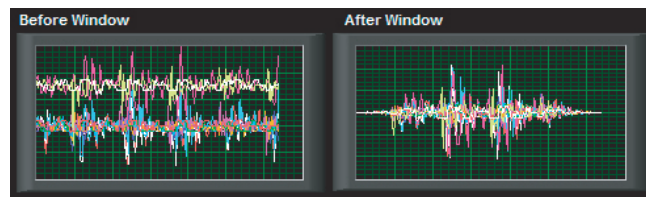


Figure 58. Typical Data Segments

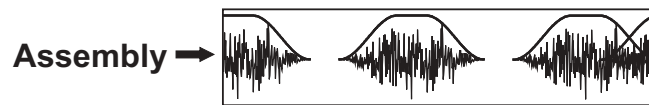


Figure 59. Assembly

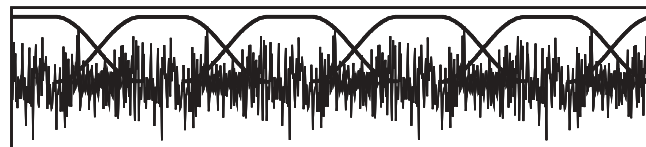


Figure 60. Assembled Planet Tooth Vector

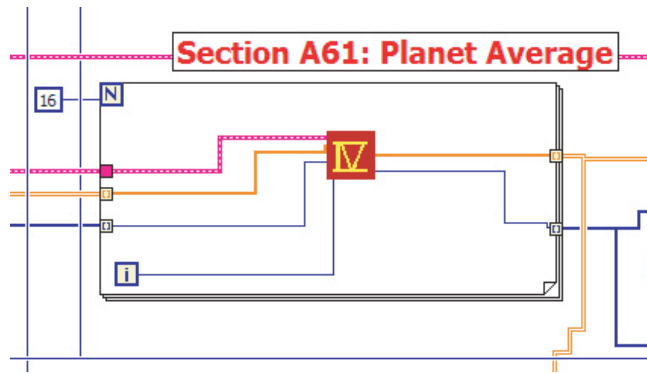


Figure 61. Section A6

Typical Output Planet Vector, (Planet1, Sensor1)

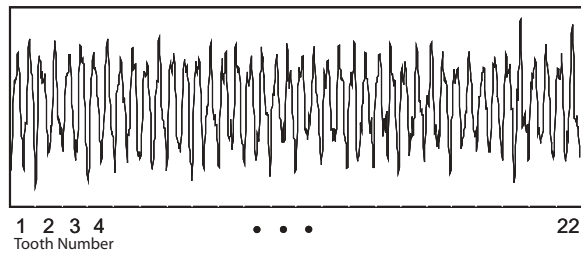


Figure 62. Typical Planet Tooth Vector (Actual Data)

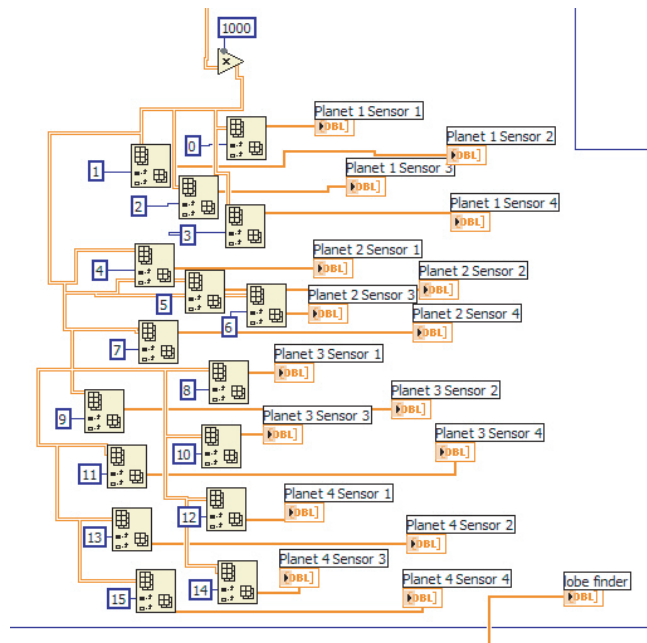


Figure 63. Display VI

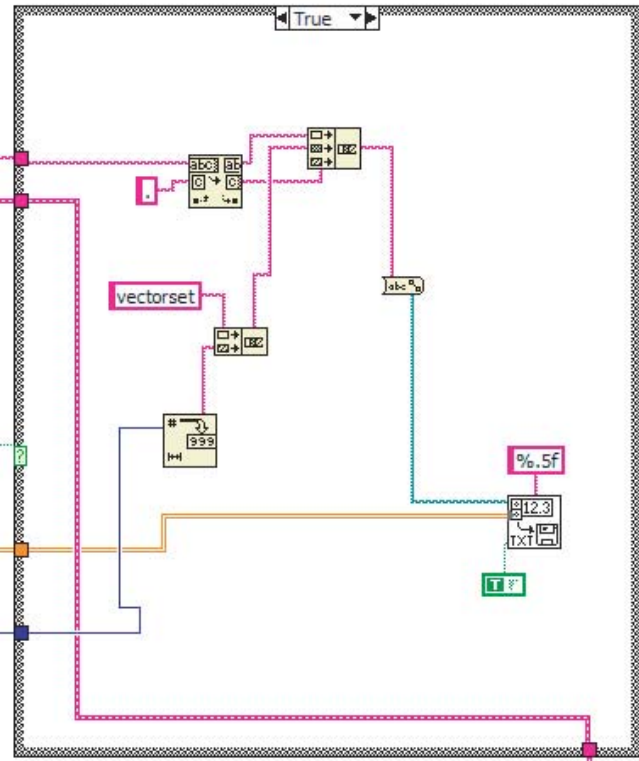


Figure 64. Output VI

After the windowing stage is the assembly stage. Each mesh window is assigned a tooth number, computed based on the geometry of the gearbox. The first mesh window is assumed to be tooth 1. Note: the hardware trigger may be used to ensure consistency in the choice of tooth 1 between runs. Each mesh window is placed into a vector associated with the proper planet in the appropriate location based on tooth number (see figure 59).

Once the vector of 1 to planet teeth assembled windows is full, as seen in figure 60, the vector is sent to the next VI and a new 1 to planet teeth vector is initialized to zero to begin the assembly process over again. The same process also occurs for the sun teeth. The sun teeth vectors use the same data segments as the planets, except the sun requires sun teeth number of data segments to fill the sun teeth vector. With more sun gear teeth than planet gear teeth, the sun will assemble fewer averages than the planet assembly.

- **Section A6:**

Here the vectors output from the assembly VI are averaged. The number of ensembles averaged before acquisition is stopped is set in number of averages if the acquisition switch is on, and is displayed in planet averages completed and sun averages completed.

Possible Options for Program

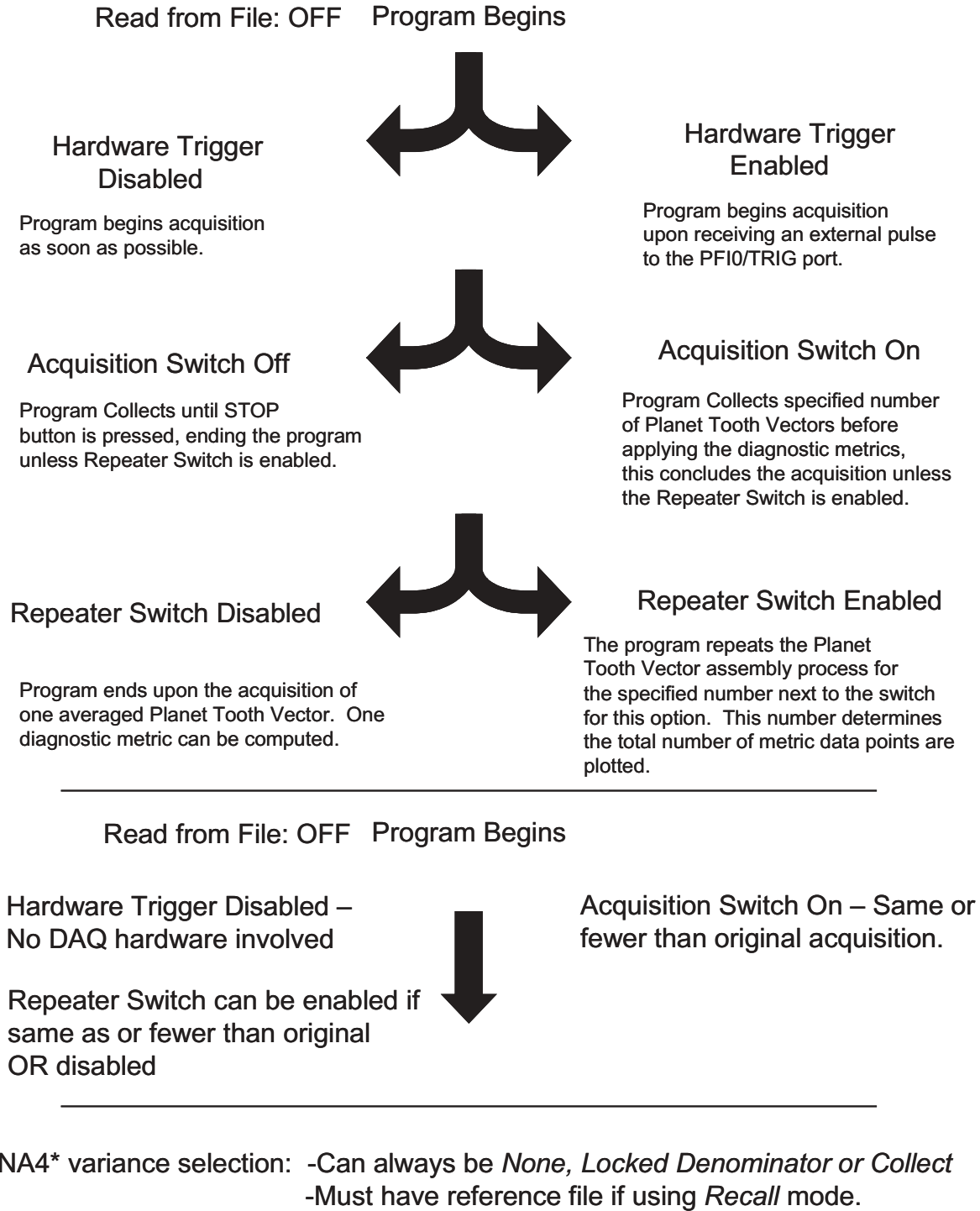


Figure 65. Program Execution Options

Notice that the loop is iterated exactly 16 times (see figure 61). This is to average every planet/sensor combination, assuming a maximum of 4 planets and 4 sensors. A typical example of a final vector that averages 25 vectors with 5 damaged teeth is shown in figure 62.

The data flow shown in figure 63 and figure 64 shows all of the averaged vectors being routed to their respective display windows. Notice that the final output vectors are scaled up by 1000 simply to bring the order of magnitude of the data into a decent range for export. The code in figure 64 accepts the final 16 planet and 16 sun teeth vectors and creates a file that can readily be read into MS Excel and Mathworks Matlab for data processing. The metrics output is also contained in the code in figure 64 in a sequence structure.

A.4. Example Acquisition

The purpose of this chapter is to show the details of a sample acquisition in order to provide the reader a clear understanding of how to setup and run the program. This test run involves three planets and four sensors. First make sure the hardware is setup properly. In this case, the hardware trigger needs to be attached to PFIO. The 1/rev pulse generator should be attached to AC channel 0 and the sensors should be attached to AC channels 1 through 4. Be sure to choose the source type appropriately, floating versus grounded. This is usually set on the BNC connection patch board, such as the BNC 2120 from National Instruments. The blue optional input section is set up as shown in figure 46. All five optional switches, speech notifications, repeater switch, save to spreadsheet file, hardware trigger, acquisition switch are enabled for this test. For this system, the trigger level must to be set to 4 volts and is attached to the PFIO BNC port. The time limit is set to 400 sec. The value of time limit is chosen simply to be more than the period of the hardware trigger. The number of planet averages desired is 25. The Repeater Switch is set to 2. With these settings, the program will acquire 2 sets of averaged teeth vectors that are saved to file. The hysteresis, additional trigger params, and input limits are left to their default values.

The pink required input section is set to the following parameters as shown in figure 44. Scan rate and scans to read are set to 12800. The pulse threshold and pulse width are set to 3.00 and 25 respectively. Note: the 1/rev pulse has a maximum amplitude of 5 volts.

In the gearbox used in this test, there are 71 ring teeth and 22 planet teeth. A mesh window of 5 teeth and a mesh period in scans of 64 scans is desired. In practice, a mesh period of 128 scans may also be used, but when set to 256 scans, a 2.2 GHz computer with 512 MB of RAM slows down considerably. If, for any reason, the computer appears to bog down, lowering the scan rate, raising the scans to read relative to the scan rate, and keeping a lower mesh period in scans should help solve the problem. Raising the scans to read relative to the scan rate will increase updating time. With these values the same, the update rate is once every second. If

scans to read is twice the value of scan rate the update will be once every two seconds. Finally, the sensor and planet input parameters are set as shown in figure 45 for the system used in this test. These values were found geometrically by inspection.

Once these inputs are set, acquisition can begin. However, it is recommended that the gearbox be allowed to reach its nominal operating RPM prior to starting acquisition. To begin acquisition, click the run selection under the Operate menu or press CTRL+R, (the shortcut keys to start a LabVIEW VI). With the speech notifications on, a voice should announce the beginning of the program. The hardware trigger on the UMD test rig pulses once every 550 rotations. Once the pulse occurs, the acquisition begins. Since the system was set to average 25 ensembles and then stop the average, save the data, and repeat, the user can stay out of the program loop for the next few minutes during the acquisition. The green windows update every 22 rotations with updated averaged data. This amounts to once every 5 or 6 seconds. The violet windows for the sun update every 25 rotations which amount to slightly higher time than the planet windows. Once the 25 planet averages and 22 sun averages are acquired, the acquisition stops, saves the data and the metrics, and waits for the next hardware pulse to begin the acquisition of another set of teeth vectors. After the second set is acquired, the data is output to the files as specified in the save to file fields, and a voice should announce the completion of the acquisition. This file is now available for a multitude of uses. A typical output as displayed on the front panel in the green planet output section and violet sun output section is shown in figure 48 and figure 50 respectively. Note the zero lines in the planet 4 columns. In this situation, zeros are still fed through the program for any sensors or planets not specified in the sensor and planet input parameters. In addition, these vectors of zeros are saved to file along with the other data and can act as a place holder when importing the file.

A.5. Future Updates

A future version of this program will include support for greater than four planets and four sensors. In addition, the program will include an adaptive lifting diagnostic algorithm designed by Paul Samuel. More statistical metrics will be added over time as well. A sister program to this, essentially a subset of the code since spur gears require no vibration separation, designed for testing spur gear damage and attempting prognosis has been developed. The new spur gear program will also eventually utilize the Constrained Adaptive Lifting algorithm as a tool for tracking damage over time.

References

- [1] P. D. McFadden and I. M. Howard. The detection of seeded faults in an epicyclic gearbox by signal averaging of the vibration. Technical Report ARL-PROP-R-183, Australian Department of Defense: Aeronautical Research Laboratory, October 1990.

- [2] P. D. McFadden. A technique for calculating the time domain averages of the vibration of the individual planet gears and sun gear in an epicyclic gearbox. *Journal of Sound and Vibration*, 144(1):163–172, 1991.
- [3] P. D. Samuel and D. J. Pines. Vibration separation and diagnostics of planetary geartrains. In *Proceedings of the American Helicopter Society 56th Annual Forum*, Virginia Beach, Va, May 2000.
- [4] R. M. Stewart. Some useful analysis techniques for gearbox diagnostics. Technical Report MHM/R/10/77, Machine Health Monitoring Group, Institute of Sound and Vibration Research, University of Southampton, July 1977.
- [5] J. J. Zakrajsek, H. J. Decker, and R. F. Handschuh. Application of fault detection techniques to spiral bevel gear fatigue data. Technical Report NASA TM-106467, ARL-TR-345, NASA and the U.S. Army Research Laboratory, January 1994.
- [6] H. J. Decker, R. F. Handschuh, and J. J. Zakrajsek. An enhancement to the na4 gear vibration diagnostic parameter. Technical Report NASA TM-106553, ARL-TR-389, NASA and the U.S. Army Research Laboratory, July 1994.
- [7] F. K. Choy, S. Huang, J. J. Zakrajsek, R. F. Handschuh, and D. Townsend. Vibration signature analysis of a faulted gear transmission system. Technical Report NASA TM-106623, NASA, 1994.
- [8] W. J. Wang and P. D. McFadden. Application of orthogonal wavelets to early gear damage detection. *Mechanical Systems and Signal Processing*, 9(5):497–507, September 1995.
- [9] W. J. Wang and P. D. McFadden. Application of wavelets to gearbox vibration signals for fault detection. *Journal of Sound and Vibration*, 192(5):927–939, May 1996.
- [10] P.D. Samuel, D. J. Pines, and D. G. Lewicki. Fault detection in the oh-58a main transmission using the wavelet transform. In *Proceedings of the 52nd Meeting of the Society for Machinery Failure Prevention Technology (MFPT)*, pages 323–335, Virginia Beach, VA, March 1998.
- [11] P. D. Samuel, D. J. Pines, and D. G. Lewicki. A comparison of stationary and non-stationary transforms for detecting faults in helicopter gearboxes. *Journal of the American Helicopter Society*, 45(2):125–136, April 2000.

- [12] M. A. Essawy, S. Diwakar, S. Zein-Sabatto, and A. K. Garga. Fault diagnosis of helicopter gearboxes using neuro-fuzzy techniques. In *Proceedings of the 52nd Meeting of the Society for Machinery Failure Prevention Technology (MFPT)*, pages 293–302, Virginia Beach, VA, March 1998.
- [13] P. D. Samuel and D. J. Pines. Classifying helicopter gearbox faults using a normalized energy metric. *Journal of Smart Materials and Structures*, 10(1):145–153, February 2001.
- [14] P. D. Samuel and D. J. Pines. Planetary gear box diagnostics using adaptive vibration signal representations: a proposed methodology. In *Proceedings of the American Helicopter Society 57th Annual Forum*, Washington, DC, May 2001.
- [15] A. Kahraman. Planetary gear train dynamics. *Journal of Mechanical Design*, 116:713–720, 1994.
- [16] W. Sweldens. The lifting scheme: A new philosophy in biorthogonal wavelet constructions. In *Wavelet Applications in Signal and Image Processing III, Proceedings of SPIE Vol. 2569*, pages 68–79, San Diego, CA, July 1995.
- [17] W. Trappe and K. J. R. Liu. Adaptivity in the lifting scheme. In *Proceedings of the Conference on Information Sciences and Systems*, pages 950–955, Baltimore, MD, March 1999.
- [18] R. L. Claypoole, R. G. Baraniuk, and R. D. Nowak. Adaptive wavelet transforms via lifting. In *Proceedings of the IEEE Conference on Acoustics, Speech, and Signal Processing*, pages 1513–1516, Seattle, WA, May 1998.
- [19] S. Braun. The extraction of periodic waveforms by time domain averaging. *Acustica*, 32(2):69–77, 1975.
- [20] H. J. Decker and J. J. Zakrajsek. Comparison of interpolation methods as applied to time synchronous averaging. Technical Report NASA TM-1999-209086, ARL-TR-1960, NASA and the U.S. Army Research Laboratory, June 1999.
- [21] Technical discussions with rotorcraft industry engineers. Technical report, 1998.
- [22] P. D. McFadden. Interpolation techniques for time domain averaging of gear vibration. *Mechanical Systems and Signal Processing*, 3(1):87–97, January 1989.
- [23] C. R. Trimble. What is signal averaging? *Hewlett-Packard Journal*, 19(8):2–7, 1968.
- [24] I. M. Howard. An investigation of vibration signal averaging of individual components in an epicyclic gearbox. Technical Report ARL-PROP-R-185, Australian Department of Defense: Aeronautical Research Laboratory, March 1991.

- [25] D. Forrester. A method for the separation of epicyclic planet gear vibration signatures. In *Proceedings of Acoustical and Vibratory Surveillance Methods and Diagnostic Techniques*, pages 539–548, Senlis, France, October 1998.
- [26] D. Blunt and D. Forrester. Analysis of epicyclic gearbox vibration. In *Proceedings of the DSTO Third International Conference on Health and Usage Monitoring - HUMS2003*, Melbourne, Australia, February 2003. Paper No. 5.10, Included on CD-ROM.
- [27] A. L. Gu, R. H. Badgley, and T. Chiang. Planet-pass-induced vibration in planetary reduction gears. Technical Report 74-DET-93, American Society of Mechanical Engineers, 1974.
- [28] P. D. McFadden and J. D. Smith. An explanation for the asymmetry of the modulation sidebands about the tooth meshing frequency in epicyclic gear vibration. *Proceedings of the Institution of Mechanical Engineers. Part C, Journal of Mechanical Engineering Science*, 199(C1):65–70, 1985.
- [29] P. D. McFadden. Window functions for the calculation of the time domain averages of the vibration of the individual planet gears and sun gear in an epicyclic gearbox. *Journal of Vibration and Acoustics*, 116:179–187, April 1994.
- [30] P. D. McFadden. On the use of windows for harmonic analysis with the discrete fourier transform. *Proceedings of the IEEE*, 66(1):66–67, January 1978.
- [31] B. D. Forrester. Method and apparatus for performing selective signal averaging. Australian Provisional Patent No. PN0234/94ARL-PROP-R-185, 1994.
- [32] B. D. Forrester. Method for the separation of epicyclic planet gear vibration signatures. U.S. Provisional Patent No. 60/102,754, 1998.
- [33] J. K. Conroy, P. D. Samuel, and D. J. Pines. Development of a real-time labview-based testbed for implementation of planetary gear diagnostic algorithms. In *Proceedings of the American Helicopter Society 59th Annual Forum*, pages 1347–1354, Phoenix, AZ, May 2003.
- [34] National instruments labview software. Website www.labview.com.
- [35] P. D. Samuel and D. J. Pines. A planetary gearbox diagnostic technique using constrained adaptive lifting. In *Proceedings of the DSTO Third International Conference on Health and Usage Monitoring - HUMS2003*, Melbourne, Australia, February 2003. Paper No. 5.9, Included on CD-ROM.

- [36] P. D. Samuel and D. J. Pines. Helicopter transmission diagnostics using constrained adaptive lifting. In *Proceedings of the American Helicopter Society 59th Annual Forum*, pages 351–361, Phoenix, AZ, May 2003.
- [37] I. Daubechies and W. Sweldens. Factoring wavelet transforms into lifting steps. *Journal of Fourier Analysis and Applications*, 4(3):245–276, 1998.

REPORT DOCUMENTATION PAGEForm Approved
OMB No. 0704-0188

Public reporting burden for this collection of information is estimated to average 1 hour per response, including the time for reviewing instructions, searching existing data sources, gathering and maintaining the data needed, and completing and reviewing the collection of information. Send comments regarding this burden estimate or any other aspect of this collection of information, including suggestions for reducing this burden, to Washington Headquarters Services, Directorate for Information Operations and Reports, 1215 Jefferson Davis Highway, Suite 1204, Arlington, VA 22202-4302, and to the Office of Management and Budget, Paperwork Reduction Project (0704-0188), Washington, DC 20503.

1. AGENCY USE ONLY (Leave blank)		2. REPORT DATE May 2004	3. REPORT TYPE AND DATES COVERED Final Contractor Report	
4. TITLE AND SUBTITLE Planetary Transmission Diagnostics			5. FUNDING NUMBERS WBS-22-714-09-16 NAS3-2223	
6. AUTHOR(S) Paul D. Samuel, Joseph K. Conroy, and Darryll J. Pines				
7. PERFORMING ORGANIZATION NAME(S) AND ADDRESS(ES) University of Maryland Alfred Gessow Rotorcraft Center Department of Aerospace Engineering College Park, Maryland 20742-0001			8. PERFORMING ORGANIZATION REPORT NUMBER E-14544	
9. SPONSORING/MONITORING AGENCY NAME(S) AND ADDRESS(ES) National Aeronautics and Space Administration Washington, DC 20546-0001			10. SPONSORING/MONITORING AGENCY REPORT NUMBER NASA CR-2004-213068	
11. SUPPLEMENTARY NOTES Project Manager, David G. Lewicki, Structures and Acoustics Division, NASA Glenn Research Center, organization code 5950, 216-433-3970.				
12a. DISTRIBUTION/AVAILABILITY STATEMENT Unclassified - Unlimited Subject Category: 37 Available electronically at http://gltrs.grc.nasa.gov This publication is available from the NASA Center for AeroSpace Information, 301-621-0390.			12b. DISTRIBUTION CODE Distribution: Nonstandard	
13. ABSTRACT (Maximum 200 words) This report presents a methodology for detecting and diagnosing gear faults in the planetary stage of a helicopter transmission. This diagnostic technique is based on the constrained adaptive lifting algorithm. The lifting scheme, developed by Wim Sweldens of Bell Labs, is a time domain, prediction-error realization of the wavelet transform that allows for greater flexibility in the construction of wavelet bases. Classic lifting analyzes a given signal using wavelets derived from a single fundamental basis function. A number of researchers have proposed techniques for adding adaptivity to the lifting scheme, allowing the transform to choose from a set of fundamental bases the basis that best fits the signal. This characteristic is desirable for gear diagnostics as it allows the technique to tailor itself to a specific transmission by selecting a set of wavelets that best represent vibration signals obtained while the gearbox is operating under healthy-state conditions. However, constraints on certain basis characteristics are necessary to enhance the detection of local wave-form changes caused by certain types of gear damage. The proposed methodology analyzes individual tooth-mesh waveforms from a healthy-state gearbox vibration signal that was generated using the vibration separation (synchronous signal-averaging) algorithm. Each waveform is separated into analysis domains using zeros of its slope and curvature. The bases selected in each analysis domain are chosen to minimize the prediction error, and constrained to have the same-sign local slope and curvature as the original signal. The resulting set of bases is used to analyze future-state vibration signals and the lifting prediction error is inspected. The constraints allow the transform to effectively adapt to global amplitude changes, yielding small prediction errors. However, local wave-form changes associated with certain types of gear damage are poorly adapted, causing a significant change in the prediction error. The constrained adaptive lifting diagnostic algorithm is validated using data collected from the University of Maryland Transmission Test Rig and the results are discussed.				
14. SUBJECT TERMS Fault detection; Transmissions (machine elements); Epicyclic gears			15. NUMBER OF PAGES 89	
			16. PRICE CODE	
17. SECURITY CLASSIFICATION OF REPORT Unclassified	18. SECURITY CLASSIFICATION OF THIS PAGE Unclassified	19. SECURITY CLASSIFICATION OF ABSTRACT Unclassified	20. LIMITATION OF ABSTRACT	

